The role of FAS in lymphoma

Stephanie Totten
Department of Experimental Medicine
McGill University, Montreal
August 2015

A thesis submitted to McGill University in partial fulfillment
of the requirements of the degree of Master of Science

© Stephanie Totten 2015

Acknowledgements

First, I would like to thank my supervisor and mentor, Dr. Nathalie Johnson for providing me with the opportunity to work on such a *FAScinating* project. I will forever be grateful for your support, your guidance and the impact you had on me. Thank you to my committee members for their advice and encouragement, to my advisor Dr. Chantal Autexier and to Dr. Marc Fabian. With a special thank you to Dr. Koren Mann, who played a fundamental role in this project, and whom I consider a great mentor. A BIG thank you to our research assistant, Dr. Maryse Lemaire for her patience, her support and her time, as well as her revisions, corrections and help translating the abstract. Without her, this thesis would not have been possible. Thank you to my colleague and friend Dr. Pierre Sesques for his help with the experiments and for the laughs. Thank you to Dr. Ana Chirigiu for her work with the lymphoma bank and her friendship. Thank you to Dr. Denis Gaucher and Hawley Rigsby for their initial work on this project and help with experiments. And thank you to Christina Weisstock for her help with the murine *Fas/FasL* expression experiment. Thank you to Dr. Alicia Bolt for her multi-colour flow cytometry staining protocol and the training. Thank you to Christian Young for the continuous FCM training, his help with compensation and data analysis. Thank you to all animal quarters staff, especially to Yvhans Chery, Kathy-Ann Forner and Veronique Michaud, not only for the trainings, for all of the laughs and memories, too.

Thank you to our collaborators: Dr. Randy Gascoyne, (British Columbia Cancer Agency, University of British Columbia), Dr. Marco A. Marra (Genome Sciences Centre, BC Cancer Research Centre, Vancouver, BC, Canada), Dr. Ryan D. Morin (Simon Fraser University, Genome Sciences Centre, BC Cancer Research Centre), Dr. Joseph M. Connors (Centre for Lymphoid Cancer, BC Cancer Agency), Dr. David Scott (Centre for Lymphoid Cancer, BC Cancer Agency), Dr. Sarit Assouline (Department of Medicine and Oncology, Jewish General Hospital, McGill University) and Dr. Saul Frenkiel (Otolaryngology - Head and Neck Surgery, Jewish General Hospital), Dr. Leon Van Kempen and Marie-Noël Boutchou (Lady Davis Institute, McGill University) for the Nanostring data and help with the analysis; Dr. Jerry Pelletier and Dr. Regina Cencic (Rosalind and Morris Goodman Cancer Research Center, McGill University) and Dr. Scott Lowe (Memorial Sloan Kettering Cancer Center) for the E*u-Myc* Model.

Thank you to the Department of Experimental medicine for the conference Travel Award. The Faculty of Medicine for the International Training Travel Award. Finally thank you to the CIHR funding agency for the Frederick Banting and Charles Best Graduate Scholarship and for the funding for this project.

Thank you, Merci, Grazie, Gracias, Dankjewel, مرتشکرم, to my dear friends at the LDI, for the great talks, the advice and the good times.

Finally, I would also like to acknowledge my family for their constant support. And to JF, for his encouragement and love.

Table of Contents

Abstract

Follicular lymphoma (FL) is usually an indolent lymphoma with a median survival of 10 to 15 years. However, ~15% of patients have a very poor outcome because their FL transformed to a more aggressive diffuse large B cell lymphoma (DLBCL) or developed early resistance to front-line chemotherapy. Identifying these patients with high-risk FL represents a currently unmet clinical need. Recent sequencing efforts have identified recurrent genetic events that contribute to the pathogenesis of FL, but their clinical significance remain unknown.

We first identified a *FAS* mutation in a patient with primary-refractory FL and subsequently found *FAS* mutations to be associated with an increased risk of histological transformation and a tendency to develop therapeutic resistance. FAS, a key death receptor in the extrinsic apoptotic pathway, plays a fundamental role in immune homeostasis by initiating apoptosis in lymphocytes once activated by FAS ligand (FASL) from neighboring cells. We confirmed that the most common *FAS* mutation, (Y232*), inhibited FAS-mediated apoptosis in lymphoma cell lines, but did not induce therapeutic resistance *in vitro*. We hypothesized that *FAS* mutations would increase tumor growth and cause therapeutic resistance *in vivo*, due to critical interactions with FASL within the tumor microenvironment that were not present in our *in vitro* model.

Using a mouse model of lymphoma, we assessed the effect of mutant FAS on lymphoma growth and chemosensitivity, and observed that a single Fas mutation significantly accelerated lymphoma growth and led to inferior response to chemotherapy in comparison to the Fas wild type lymphoma. However, the Fas mutant phenotype was no longer significant when the same cells were injected in immunosuppressed mice, suggesting that FAS-FASL interactions between tumor cells and the microenvironment are important in controlling lymphoma growth. Finally, to gain more insight into the biology of human *FAS*-mutant lymphomas, we compared the gene expression profiles of *FAS*-mutant *versus FAS*-wild-type lymphomas that were obtained from patients with relapsed refractory DLBCL, and found that *FAS*-mutant lymphomas have a potential regulatory B cell phenotype, that may allow them to overcome anti-tumor immune mechanisms and confer these cancer cells with an advantage for survival. A better understanding

of the involvement of *FAS* mutations and their interactions with the microenvironment could lead to identification of novel therapeutic targets from which patient could benefit.

Abrégé

Le lymphome folliculaire (FL) est un lymphome indolent qui présente une survie moyenne de 10 à 15 ans. Par contre, environ 15% des patients atteint de FL voit leur situation s'aggraver, soit par l'évolution de la maladie en une forme plus agressive, à savoir le lymphome diffus à grandes cellules B (DLBCL), ou encore en développant une résistance à la chimiothérapie de première ligne. Pouvoir identifier ces patients à haut risque permettrait de mieux les traiter. Des efforts de séquençage des cellules cancéreuses de ces patients ont récemment permis d'identifier certains génotypes qui contribuent à la pathogénèse du FL, sans pour autant qu'on comprenne leur pertinence clinique.

Nous avons identifié une mutation dans le gène *FAS* chez des patients présentant un FL réfractaire, et nous avons subséquemment observé que cette mutation est associée non seulement à une augmentation du risque de transformation vers DLBCL, mais aussi avec un propension à favoriser la chimiorésistance. FAS est un récepteur de mort cellulaire important impliqué dans l'apoptose; il joue un rôle fondamental dans l'homéostasie du système immunitaire en initiant les fonctions apoptotiques de cellules préalablement activés par le ligand de FAS (FASL), qui lui provient du microenvironnement. Nous avons confirmé que la mutation de FAS la plus fréquente, (Y232*), empêche cette réaction, sans pour autant induire une chimiorésistance *in vitro*. Nous émettons donc l'hypothèse que les mutation de *FAS* favorisent l'augmentation de la croissance tumorale et induisent la résistance aux agents chimiothérapeutiques.

À l'aide d'un modèle murin de lymphome, nous avons évalué les effets qu'a une mutation du gene FAS sur la croissance et la sensibilité chimiothérapeutique du lymphome. Nous avons observé qu'une mutation de FAS accélère significativement la croissance du lymphome, et celui-ci réponds moins au traitement. Par contre, l'injection de ces mêmes cellules dans des souris immuno-supprimées suggère que les interactions qu'ont FAS et FASL entre la tumeur et le microenvironnement sont importantes pour contrôler la croissance du lymphome. Finalement, pour mieux comprendre la biologie et le rôle d'une mutation de FAS chez l'humain, nous avons comparé le profil d'expression génique de cellules présentant une mutation de FAS ou non, provenant de biopsies de lymphomes obtenues de patients avec une rechute d'un lymphome

réfractaire au traitement. Nous avons observé que les patients ayant une mutation de FAS présentent un phénotype potentiel de cellulles B régulatoires, favorisant ainsi la survie de ces cellules. Une meilleure compréhension des conséquences des mutations dans le gène FAS, ainsi que de l'implication de l'interaction des cellules cancéreuses avec le microenvironnement pourraient permettre l'identification et l'utilisation de nouvelles thérapies desquels le patient pourrait bénéficier.

Preface & Contribution of Authors

The following is my Master's thesis entitled "The role of FAS in lymphoma" which is composed of 4 chapters in accordance to the guidelines outlined by the Department of Graduate and Postdoctoral Studies. In addition to the core elements of my thesis presented in Chapter 1 (Literature review), Chapter 2 (Introduction, Hypothesis, Methods, Results, Figures and Discussion) and Chapter 4 (Conclusion and Summary), a short report outlining my work optimizing an *in vivo* imaging model is included in Chapter 3. The contributions of each author are described below.

The majority of the experiments and analysis were performed by Stephanie Totten.

Previous experiments discussed in the introduction and used as basis for this project, were performed by Dr. Nathalie Johnson and Dr. Denis Gaucher. Dr. Denis Gaucher also performed the experiment in Figure 2.1B.

Dr. Pierre Sesques and Christina Weisstock helped with the *Fas/Fasl* microenvironment mouse experiment (Figures 2.4).

The patient cell lines used in Figure 2.5 were developed and characterized by Dr. Ana Chirigiu, Dr. Maryse Lemaire and Dr. Denis Gaucher as part of the BCLQ.

The RNA extraction from patient lymphoma samples and the microarray analysis were performed by our QCROC2 partners, as part of the QCROC2 trial. The treatment of the BJAB cell lines with CH-11 was performed by Dr. Denis Gaucher. The nanostring experiments were performed by Marie-Noël Boutchou, and Dr. Leon Van Kempen helped with the nanostring data analysis (Figure 2.6). Dr. Koren Mann also helped with the analysis in Figure 2.6.

List of Figures

List of Tables

Abbreviations

ABC: Activated B cell like
APAF-1: Apoptotic protease activating factor 1
AID: Activation-induced deaminase
ALPS: Autoimmune lymphoproliferative syndrome
ASPP2: Apoptosis-stimulating of p53 protein 2
BAD: Bcl-2-associated death promoter
BAK: Bcl-2 homologous antagonist/killer
BAX: Bcl-2-associated X protein
BCL2: B-cell lymphoma 2
BCL6: B-cell lymphoma 6
BCLQ: Banque de cellules leucémique du Québec ("Quebec Leukemia Cell Bank")
BCL-XL: B-cell lymphoma-extra large
BCL-W: Bcl-2-like protein 2
BCS: Body condition score
Bfl-1/A1: Bcl-2 related protein 1
BH3: Bcl-2 homology domain 3
BID: BH3 interacting-domain death agonist
BIK: Bcl-2 interacting killer protein
BLI: Bioluminescence imaging
BIM: Bcl-2 interacting mediator of cell death
BMF: Bcl-2-modifying factor
CAD: Caspase-activated deoxyribonuclease
CD: Cluster of differentiation
CRD: Cysteine-rich domain
CTL: Cytotoxic T lymphocyte
DD: Death domain
DISC: Death-inducing signaling complex
DLBCL: Diffuse large B cell lymphoma
DR3-5: Death receptors 3-5
DRM: Detergent resistant micro-domains
EZH2: Enhancer of zeste homolog 2
EP300: E1A binding protein
ER: Endoplasmic reticulum
FACS: Fluorescence-activated cell sorting
FADD: FAS-associated death domain protein
FAS: Human FAS Protein
FAS: Human FAS gene
Fas: Mouse FAS transgene
Fasl: Mouse FAS ligand transgene
Fas: Mouse FAS gene when part of genome
Fasl: Mouse FAS ligand gene when part of genome
FCM: Flow cytometry
FDR: False-discovery rate
FL: Follicular lymphoma

FMO: Fluorescence minus one control
GC: Germinal center
GCB: Germinal centre B-cell-like
GFP: Green-fluorescent protein
GSEA: Gene set enrichment analysis
GZMB: Granzyme B
HDACi: Histone deacetylase inhibitor
HME: Histone-modifying enzymes
HMGB1: High mobility group box 1
HRK: Activator of apoptosis harakiri
ICAD: Inhibitor of caspase-activated deoxyribonuclease
ICD: Immunogenic cell death
iMEF: Irradiated murine embryonic fibroblast
IgH: Immunoglobulin heavy locus
IRES: Internal ribosome entry site
IP: Intraperitoneal
IPA: Ingenuity Pathway Analysis
IV: intravenous
IVIS: *In vivo* imaging system
MCL-1: Induced myeloid leukemia cell differentiation protein
MEF: Murine embryonic fibroblast
MFI: Mean fluorescence intensity
MSCV: Murine stem cell virus
MOMP: Mitochondrial outer membrane permeabilization
MYCL Myelocytomatosis viral oncogene homolog
NHL: Non-Hodgkin lymphoma
NOXA: Phorbol-12-myristate-13-acetate-induced protein
PARP: Poly (ADP-ribose) polymerase
PCD: Programmed cell death
PUMA: p53 upregulated modulator of apoptosis
QCROC: Quebec Clinical Research Organization in Cancer
R-CVP: Rituximab, cyclophosphamide, prednisone
R-CHOP: Rituximab, cyclophosphamide, hydroxydaunorubicin, oncovin, prednisone
rrDLBCL: Relapsed/refractory diffuse large B cell lymphoma
SS: Single-Stained control
TLy: Transformed lymphoma
TM: Transmembrane
TNF: Tumor necrosis factor
TNF-R1: Tumor necrosis factor receptor 1
TP53: Tumor protein p53
TP53BP2: Tumor Protein P53 Binding Protein 2
TRADD: TNF-R1 associated death domain protein

Chapter 1: Literature Review

1. Non-Hodgkin Lymphoma

The 5th most common cancer in Canadians is non-Hodgkin lymphoma (NHL), which consists of a diverse group of hematological cancers derived from lymphocytes[1]. There are both indolent and aggressive forms of NHL, where follicular lymphoma (FL) and diffuse large B cell lymphoma (DLBCL) are respectively the most prevalent of each type[2].

1.1. Follicular lymphoma

FL is the second most common NHL worldwide, and the most common subtype in Canada, representing about 32% of all cases (Figure 1.1). FL results from the malignant transformation of normal germinal center (GC) B cells, where GCs are compartments within secondary lymphoid organs and are the site of *clonal expansion, somatic hyper-mutation and selection of B cells*[3,4].

1.1.1. Clinical features

Patients with FL typically present with lymphadenopathy, with or without B symptoms, which include fever, weight loss, and persistent night sweats[5]. Histologically, FL is typically characterized by the arrangement of cells in tightly packed follicles within the lymph node. The main cell type in these follicles is the small cleaved follicle center cell (centrocyte) however, non-cleaved large follicle center cells (centroblasts) are also always present in FL[6]. The follicles are also surrounded by non-malignant cells, including T cells, dendritic cells and macrophages[7]. The clinical course of FL is usually indolent, where a "watch and wait" approach is used for the management of disease for patients who are asymptomatic and have low tumor burden . Yet, for patients with low grade disease whom present with or eventually develop symptomatic disease and/or a high tumor burden, the management of the disease can consists of radiation therapy ;. For those with higher grade disease[8], the combination of cytotoxic chemotherapy and the monoclonal CD20 antibody, rituximab, are used. Two common chemotherapeutic

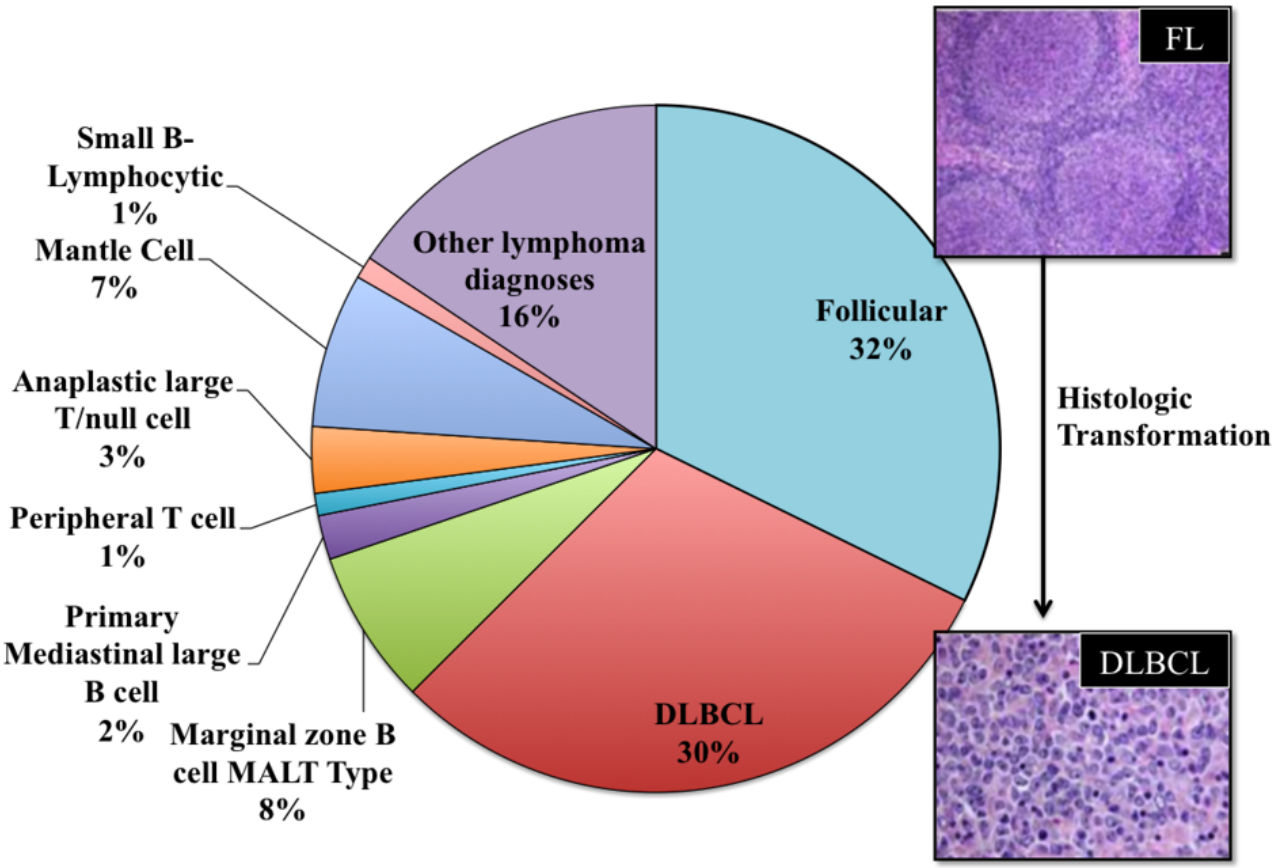

Figure 1.1. NHL subtypes and incidences.
FL and DLBCL are the most prevalent. FL can undergo histologic transformation to DLBCL. Adapted from Anderson et al.[2] and, Lossos and Gascoyne[9].

regimens for the treatment of FL are R-CVP (rituximab with cyclophosphamide, oncovin (vincristine) and prednisone); and R-CHOP (rituximab with cyclophosphamide, hydroxydaunorubicin (doxorubicin), oncovin (vincristine) and prednisone), though rituximab therapy may also be used as a single agent. The outcomes of patients with FL depend on the duration of the response to chemotherapy and are extremely heterogeneous, where some patients have prolonged survival beyond 10 years and others experience rapid disease progression, or their FL undergoes histologic transformation to DLBCL[10]. In spite of improvements in therapy and increases in overall survival, FL remains a largely incurable disease as the vast majority of patients will relapse.

1.1.2. Biology of FL

The t(14;18) (q32; q21) translocation is a hallmark of FL, occurring in over 85% of cases[3]. This translocation juxtaposes the IgH gene at 14q32 and the BCL2 oncogene at 18q21 resulting in the overexpression of the anti-apoptotic protein BCL2, which impairs the normal germinal center apoptotic program[3]. This translocation is recognized as an early event that arises in the bone marrow[11]. Translocations that result in the overexpression of the anti-apoptotic protein, BCL-6 have also been reported in FL[12]. BCL-2 overexpression alone will not cause FL, as the t(14;18) translocation is found in healthy individuals as well[13]. However, overexpression of BCL2 blocks apoptosis and sets the stage for acquisition of additional secondary genetic alterations that lead to overt FL. FL-precursor cells with the IgH-BCL-2 translocation are thought to then migrate to the lymph nodes, where in some cases they gain additional mutations[14]. Constitutive expression of the activation-induced deaminase (AID) is believed to play an important role in FL development[15,16]. In normal non-malignant B cell development AID causes mutations in DNA through the deamination of the cytosine base, which plays a key role in somatic hypermutation required for diverse antibody production. However, it is postulated that inappropriate activity of AID in FL precursor cells that overexpress BCL-2, can lead to genetic instability and an accumulation of other chromosomal abnormalities[17]. FL cells have been described to have an average of four to six additional genomic alterations[18]. Some of these include duplication of the X chromosome, break in chromosome 1, deletions in chromosome 6, trisomy 7 and trisomy 12 (reviewed)[19]. Recent whole genome sequencing of FL revealed mutations in genes including

EZH2, *CREBBP*, *EP300* and *MLL2*[20,21]. FLs are extremely genetically heterogeneous, and it is this diversity that is believe to contribute to the wide spectrum of clinical courses and outcomes. Emerging evidence has revealed, that in addition to the genetic landscape, FL is also driven by critical interactions with immune cells within the tumor microenvironment, and that the particular interactions can be predictive of clinical outcome[22].

1.1.3 Tumor microenvironment in FL

FL is characterized by the presence of malignant GC B cells surrounded by a prominent microenvironment consisting of non-malignant T cells subsets, macrophages and follicular dendritic cells[3]. FL growth is driven by both genetic alterations and interactions with the immune and stromal cells within the tumor microenvironment[3]. FL is understood to rely heavily on growth and survival signals from non-malignant cells in the microenvironment, a concept that was termed "re-education" by Gascoyne[23]. The particular arrangement and type of the cells in the FL microenvironment has been compared with non-malignant GCs, including follicular T helper cells and dendritic cells; in comparison to complete destruction of the normal GC structure found in aggressive NHLs, like Burkitt's lymphoma and DLBCL[23]. Burkitt's lymphoma is primarily caused by Epstein-Barr virus and is characterized by *MYC* overexpression found in the majority of cases. In spite of a highly aggressive clinical course, patients with Burkitt's lymphoma have very high response rates to chemotherapy[24]. In comparison to DLBCL and Burkitt's lymphoma, efforts to culture FL have been largely unsuccessful, which has been recognized by many as evidence for the dependence of FL on cells in its surrounding microenvironment for growth signals, particularly from T follicular helper cells and macrophages[23]. In addition, infiltration of FL by T cells is associated with a favorable outcome whereas infiltration by macrophages may be associated with an inferior survival[22].

1.2. Transformation of FL to DLBCL

Part of the natural history of FL is the histologic transformation to the more aggressive NHL, DLBCL occurring at a rate of 3% per year[25]. There is no single driver mutation that leads to

transformation of FL. Instead, several genetic alterations have been associated with and are believed to contribute to histologic transformation of FL. Common secondary genetic alterations in FL that have been shown to contribute to histologic transformation are inactivating mutations in the tumor suppressor *TP53*, the loss of expression of the tumor suppressor p16/INK4[26] and also, MYC overexpression[17,18]. P53 is a transcription factor that responds to a variety of cellular stress signals, including DNA damage, by leading to cell-cycle arrest or even cell death. P53 also plays an important role in chemotherapy-induced cell death. P53 is frequently mutated in many different types of cancers, and lymphomas are no exception (reviewed)[27,28]. P53 mutations are not only associated with transformation, but also with poor survival[29]. In addition, mutations in epigenetic regulators including EP300 and EZH2, and in the death receptor *FAS*, were recently reported in TLy (transformed lymphoma), and proposed to also contribute to histologic transformation[30].

1.2.1 Biology and treatment of de novo DLBCL

DLBCL is characterized by an aggressive clinical course and can be divided into two types based on the cell of origin, either germinal center B-cell like (GCB) and or activating B cell–like (ABC) subtypes [31]. Unlike FL, patients with DLBCL require immediate treatment. The primary treatment is R-CHOP, which is effective in inducing remission in about 85% of patients with *de novo* DLBCL[32]. The genetic alterations in *de novo* DLBCL have been well-characterized, and include mutations in histone modifying genes, mutations within the B cell receptor (BCR) pathway that lead to increased cell survival, and finally, mutations in cell surface receptors that allow lymphoma cells to escape immune surveillance (reviewed)[33]. Murine models of disease have allowed us to gain insight into the biology of lymphoma. The most commonly used model of B cell lymphoma is the E*μ*-*Myc* model. In this model, the *Myc* gene is placed under the control of IgH Enhancer, leading to the B-cell-specific overexpression of the c-myc oncogene, a transcription factor that activates expression of genes involved in cell proliferation and resistance to apoptosis [34]. These mice develop lymphoma with 100 % incidence rate[35,36]. This model has been used to identify genes that alter the onset of lymphoma and the response to single-agent chemotherapy, including doxorubicin[37]. In spite of improvements in therapy, unfortunately a

poor initial response or early relapse after R-CHOP, and is associated with a poor survival. A subset of these patients have so called "double hit" lymphomas, where *BCL-2* and *MYC* are aberrantly expressed, which is associated with a very poor prognosis[14].

1.3. Treatment of relapsed refractory lymphoma (rrDLBCL) and transformed lymphoma (TLy)

Although progress has been made in the development of effective therapies for patients with FL, poor initial responses and relapses after rituximab and conventional chemotherapy continue to negatively affect the prognosis of many patients[3-5]. The treatment for relapsed refractory rrDLBCL and TLy is first more chemotherapy, and if necessary this is followed by autologous stem cell transplant. Enrolment in clinical trial is an option for patients with rrDLBCL (including TLy) who fail other treatments. One such trial is the "Quebec Clinical Research Organization in Cancer" (QCROC-2) (NCT01238692) phase II clinical trial. The rationale for this study was that histone deacetylase inhibitors (HDACi) may be preferentially effective in lymphomas that have mutations in histone modifying enzymes (HME)[33]. HDACi are also being tested in other cancers, and have shown to be effective in the treatment of some relapsed refractory cutaneous T cell lymphomas[38,39]. As part of this trial, biopsies acquired at the time of accrual were submitted for exome sequencing, in order to characterize the genetic alterations in rrDLBCL. The specific genes sequenced as part of this trial, included *FAS*, which is relevant to this project.

2. Apoptosis

Apoptosis is an active form of programmed cell death (PCD) that is necessary in a variety of physiological processes, including immune system homeostasis and development, and is deregulated in many cancers[40]. Apoptosis is characterized by a variety of cellular structural changes including cell shrinkage, nuclear fragmentation, chromatin condensation and fragmentation, and membrane blebbing. The small resulting structures are then phagocytized by neighboring cells or processed by the lysosome[41].

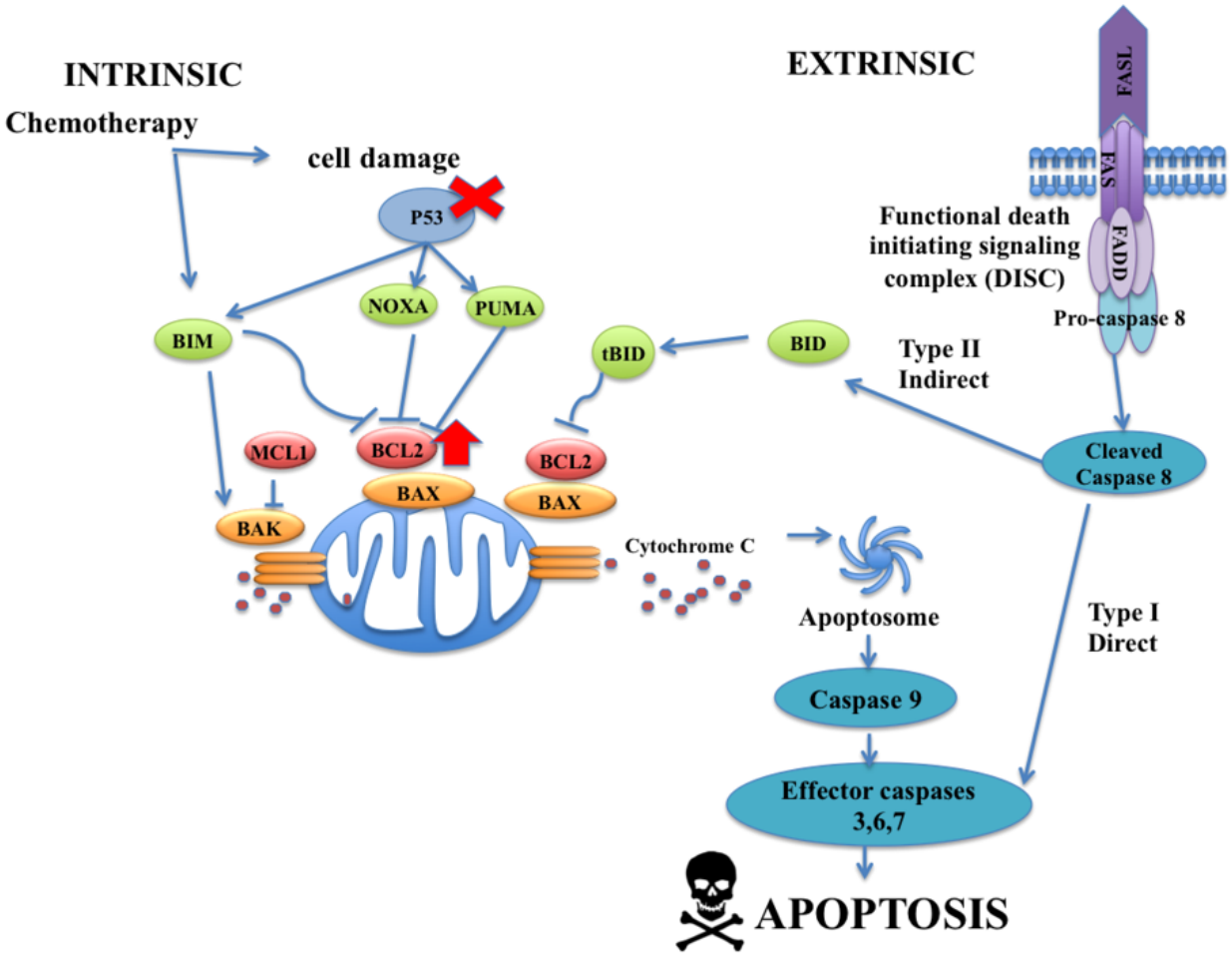

Figure 1.2. Overview of the intrinsic and extrinsic apoptotic pathways.
FAS signaling pathway is used to demonstrate key features of the extrinsic apoptotic pathway. Common blocks in intrinsic pathway of apoptosis observed in FL, such as *TP53* inactivating mutations or *BCL-2* overexpression, are also illustrated. Adapted from Vucic et al.[80].

Apoptosis is energy-dependent, and is mainly regulated through the intrinsic and extrinsic pathways. The intrinsic pathway is activated in response to ultraviolet radiation or DNA damage. The extrinsic pathway is induced by death signals, for example, from cells from the immune system in response to a virally-infected cell[42]. In addition to these two pathways, there is also a mechanism of apoptosis that involves T cell cytotoxicity and relies on perforin (a cytolytic protein) and either Granzyme A or B (which are serine proteases)[43]. The end result of the intrinsic, extrinsic and Granzyme B-dependent pathways of apoptosis are the same, they lead to caspase-3 activation which in turn results in the hallmark structural changes associated with apoptosis, and ultimately, cell death[44]. Granzyme A depends on an alternate caspase-independent pathway that is beyond the scope of this literature review[45].

Caspases are cysteine-dependent proteases that are expressed in the cell, in their inactive monomeric pro-enzyme form. They often require cleavage and/or dimerization for their activation, where active caspases have proteolytic activity[46]. Caspases that are involved in apoptosis include caspases-3, -6, -7, -8, -9 and -10, and these are subclassified by their role. caspase-8, -9 and -10 are initiator caspases that cleave and activate the effector caspase-3, -6, and -7[47]. These effector caspases, also referred to as "executioner" caspases cleave various cellular substrates including poly ADP-ribose polymerase (PARP), cytoplasmic endonucleases, cytokeratins and others that are necessary in apoptosis. Caspase-3 is the most important of the executioner caspases, as it is activated by all initiator caspases. Caspase-3 causes cytoskeletal rearrangements; activation of the endonuclease caspase-activated deoxyribonuclease (CAD) by cleaving its inhibitor (ICAD), leading to degradation of chromosomal DNA; and blebbing of the cell that are all that required for completion of the apoptotic program[48].

2.1. Intrinsic apoptosis

The intrinsic apoptotic pathway is activated in response to DNA damage caused by radiation, toxins, and most chemotherapeutic agents, and is mediated by p53 (reviewed)[49]. Intrinsic cell death is regulated at the mitochondria, and involves changes in the levels and interactions between more than twenty members of the BCL-2 family of proteins[50]. BCL-2 family members can be defined based on their function, where the first group is referred to as

effectors, and includes BAX and BAK that undergo conformational change upon activation by members of a second group referred to as the activators, BID and BIM[51,52]. Activation of BAX and BAK causes mitochondrial outer membrane permeabilization (MOMP) which is considered to be the critical step at which point the cell is irreversibly committed to PCD, ultimately leading to cytochrome C release into the cytoplasm where it can interact with the apoptotic protease activating factor (APAF-1) to form the apoptosome. This leads to the activation of caspase-9, triggering downstream cleavage and activation of the effector caspase-3, and the final stages of apoptosis.

There are also anti-apoptotic BCL-2 family member proteins, including Bcl-2, Mcl-1, Bcl-xl, Bcl-w, and Bfl-1/A1. The anti-apoptotic proteins, such as Bcl-2, bind to and sequester the activator proteins, preventing the activation of their effectors, BAX and BAK, therefore preventing MOMP. Anti-apoptotic proteins are up-regulated in many cancer types, including chronic lymphocytic leukemia, cutaneous melanoma, neuroblastoma, breast adenocarcinoma, colorectal adenocarcinoma and prostate cancer (reviewed)[53]**.** As previously discussed, Bcl-2 is overexpressed in the majority of FL cases.

Finally there are sensitizer Bcl-2 family members that are unable to induce activation of BAX and BAK directly, but instead these proteins exert their pro-apoptotic function by competing for the BH3 binding domain with anti-apoptotic proteins, and displacing or preventing the binding of activators to this site. These sensitizers include BAD, BIK, NOXA, BMF, HRK, and PUMA (Figure 1.2).

2.2. Extrinsic apoptosis

The extrinsic pathway is initiated through the stimulation of members of the tumor necrosis factor receptor (TNF-R) superfamily on the cell membrane, by their respective ligands usually bound on the surface of other cells, such as a cytotoxic T lymphocytes (CTLs)[54]. The TNF-R superfamily are type 1 transmembrane (TM) proteins that include the well-characterized FAS, TNFR1, DR3, DR4 and DR5. These receptors share conserved sequences, including the intracellular domain, called the death domain (DD) and cysteine-rich domains (CRDs) in their

extracellular domain[55]. The extrinsic pathway is induced when the cell surface death receptors, for example FAS or TNF-R1 interact with their ligands FAS ligand (FASL) and TNFα, respectively, leading to the cleavage and activation of caspase-8[50]. More specifically, ligand binding to the receptors results in their oligomerization, and the recruitment of adaptor proteins, either the FAS-associating death domain containing adaptor protein (FADD) to FAS, and/or TNF-R1 associated death domain protein (TRADD) to TNF-R1. The receptor binding to its adaptor proteins recruits the initiator caspase-8 (in its procaspase form), creating the complex known as the death-inducing signaling complex (DISC)[56,57]. The DISC formation results in procaspase-8 oligomerization and self-activation, and ultimately the cleavage of downstream effector caspases, including caspases-3, -6, -7, and the completion of the apoptotic program[58] (Figure 1.2).

3. FAS

FAS was first identified in 1989, when two separate groups found that apoptosis was induced in cells treated with two independently generated monoclonal antibodies, which they named Fas[59] and Apo-1[60]. A couple years later, *FAS* (also CD95 or Apo-1) was cloned for the first time[61]. The human *FAS* gene consists of 9 exons that encode for an N-terminal extracellular domain, a single transmembrane domain (TM), encoded by exon 6, and a cytoplasmic domain, that contains the DD (exon 9) (Figure 1.3). The extracellular domain consists of 3 CRD domains that are essential in the recognition of FASL, and is highly glycosylated[62]. Its TM domain is short consisting of only 17 amino acids[62]. Finally, the DD within the C-terminal tail of the protein consists of 6 alpha-helices that are necessary for FAS apoptotic signaling[63]. Today, *FAS* is understood to be expressed on in a variety of tissues and cell types, including activated T and B cells, hepatocytes, as well as ovarian and mammary epithelial cells[64,65]. In contrast, constitutive *FASL* expression is reported to be limited to the testis, the lung and the eye, and high levels have been reported on activated T and NK[66,67]. FAS is also understood to play key roles in immune cell homeostasis, where FASL on T and NK lymphocytes binds to FAS and initiates apoptosis in infected or auto-reactive *FAS*-expressing B cells[68].

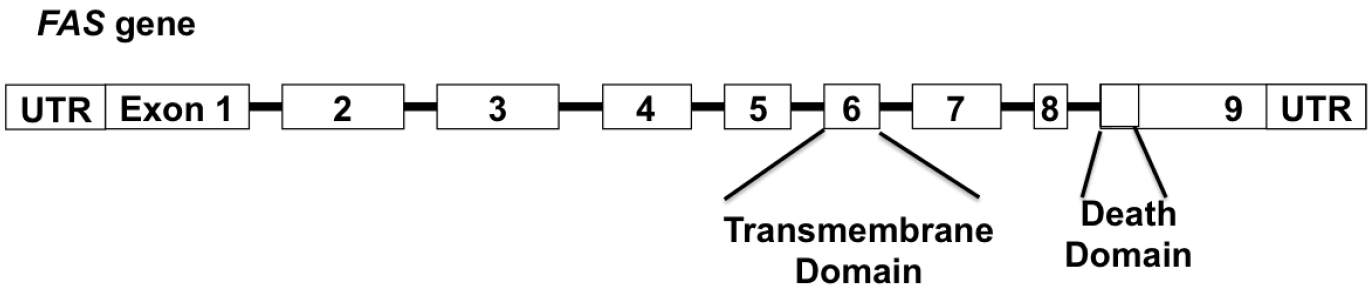

Figure 1.3. The *FAS* gene.
Adapted from Fouque et al.[68].

3.1. Role in apoptotic signaling

FAS initiates extrinsic apoptotic signaling once it is activated by FAS ligand (FASL) from surrounding cells[70,71]. The binding of FASL causes the oligomerization of 5-7 FAS receptors[72] leading to the formation of a functional DISC that consists of the recruitment of FADD and procaspase-8, through critical interactions at the FAS functional DD[73]. Procaspase-8 can then bind and activate other procaspase-8 molecules.

Cells can be divided into two groups based on their FAS apoptotic signaling, where, in type I cells, caspase-8 levels are high enough to directly activate effector caspases (caspases-3, -7 and 10). Yet, in type II cells, however, the amount of active caspase-8 generated at the DISC is not sufficient to activate effector caspase-3 directly, and instead, it potentiates the intrinsic apoptosis pathway by cleaving BID into its active form tBID, that is capable of causing cytochrome C release from the mitochondria. As in the intrinsic pathway, cytochrome C then interacts with proteins such as APAF-1, to form the apoptosome which leads to the cleavage and activation of procaspase-9 to produce active caspase-9. Caspase-9 then cleaves caspase-3, which activates CAD in the same way as it does in type I cells [74].

It has been shown that FAS-mediated apoptotic signaling can be in part regulated by the distribution of the FAS receptor within special compartments of the plasma membrane, termed detergent resistant micro-domains, also referred to as lipid rafts (DRMs)[75]. They have distinct structural composition and are understood to favor protein-protein interactions necessary in signaling pathways[76]. FAS is mostly excluded from these lipid rafts in inactivated cells, but it was shown that T cell receptor (TCR)-dependent reactivation of T cells leads to rapid distribution of the FAS into lipid rafts[77]. Furthermore, FAS clustering reduces the apoptotic threshold and favors DISC formation, and consequent induction of the apoptotic program[78]. Interestingly, the reorganization of FAS into DRMs was also found to occur after exposure to rituximab and other chemotherapeutic agents[79].

3.2. FAS/FASL signaling in cancer

A recently recognized hallmark of cancer is the ability of cancers to evade the immune system[80]. Cancer immunosurveillance encompasses the immune mechanisms that function to protect a host against cancer development, which have been shown to rely in part on *FASL* expression on the surface of CD8+ T cells, which targets cancer cells by initiating the extrinsic apoptotic pathway[81,82]. Along this line, a recent publication by Afshar-Sterle *et al* showed that $CD8^+$ cytotoxic T lymphocytes (CTLs) prevent the development of spontaneous B cell lymphoma in mice in a FASL-dependent manner[83]. Indeed FAS-FASL interactions play important in roles in tumor immunosurveillance, and some tumors have developed ways to circumvent this. For example some cancers express *FASL* to counteract tumor immunosurveillance mechanisms by killing immune cells[84,85]. Certain others rely on the loss of function of the FAS-FASL pathway to evade tumor immunosurveillance mechanisms. This includes a second hallmark of cancer, which is the ability of malignant cells to resist cell death signals[80]. The loss of function of FAS has been described in multiple cancer models and has been reported to occur by multiple mechanism including down-regulation of *FAS* expression by promoter methylation, transcriptional repression[86] and decreased histone acetylation[87]; selective production of the alternatively spliced soluble variant of FAS[88]; and the presence of inactivating *FAS* mutations[73]. FAS expression has been associated with a favorable outcome in DLBCL[89].

3.3. FAS/FASL in response to chemotherapy

A tumor's apoptotic response to chemotherapeutic agents is an important determinant of chemotherapeutic sensitivity[90,91]. Chemotherapy has been largely recognized to kill cancer cells, including lymphoma, by triggering the intrinsic apoptotic pathway[92]. Indeed, cyclophosphamide and doxorubicin, two components of R-CHOP, have been shown to elicit a DNA damage response through P53, which activates pro-apoptotic BH3 proteins[93]. However, it has been reported that cancer cells can also be killed by chemotherapy through FAS[94]. Up-regulation of *FAS* has been recognized as a key response feature of cells treated with certain cytotoxic drugs[94].

Furthermore, clinically relevant concentrations of doxorubicin, and other chemotherapies, were shown to initiate apoptosis in primary leukemia cells in a FAS-FASL-dependent manner[95].

Once understood to induce immunologically silent apoptosis of tumor cells, certain conventional chemotherapies have recently also been shown to instead elicit a form of tumor cell death that stimulates an effective T-cell mediated anti-tumor immune response[96]. Established by Kroemer and Zitvogel groups, this concept, referred to as immunogenic cell death (ICD), was demonstrated to significantly contribute to the overall efficacy of doxorubicin[97]. Using carcinogen-induced and transplantable tumor models, the successful activation of a tumor-specific immune response with inducers of ICD (such as the anthracycline doxorubicin) has been determined to depend on the ability of dying cancer cells to expose calreticulin on their outer membrane, and release ATP and the high mobility group box 1 (HMGB1) protein[98]. First, the ATP released as a result of autophagy, acts as a "find me" signal for dendritic cells, which facilitates their recruitment into the tumor microenvironment[99,100]. Second, pre-apoptotic exposure of calreticulin on the outer leaflet of the plasma membrane of dying cells, a result of the endoplasmic reticulum (ER) stress response acts as an "eat me" signal for dendritic cells[97]. Finally, the release of the nuclear HMGB1 protein from dying cells has been shown to stimulate antigen presentation to T cells[101]. Ultimately, successful ICD induction results in the re-establishment of a T-cell-mediated and interferon-gamma-based anti-tumor response[102]. CTLs are recognized as major players in the anti-tumor immune response elicited by ICD inducers, that elicit their anti-tumor cytotoxic effects through either the FAS-FASL or the perforin-Granzyme B pathways (reviewed)[103].

3.4. Dominant negative role of FAS in autoimmune lymphoproliferative syndrome

Germline *FAS* mutations have been reported in the majority of cases of autoimmune lymphoproliferative syndrome (ALPS)[104]. Patients with ALPS exhibit benign splenomegaly and massive chronic lymphadenopathy, often develop autoimmunity, and display an increased risk of developing Hodgkin and non-Hodgkin lymphoma[105]. The majority of mutations in patients with ALPS are heterogeneous and cluster to the *FAS* DD [105]. Many of these mutations have been well characterized and shown to have a dominant negative effect on FAS signaling, meaning that only

one copy of the mutated allele needs to be present for the phenotype. More specifically, the mutant FAS protein from one allele interferes with the function of the non-mutated protein encoded on the wild-type allele[106].

There are also two murine models wherein the FAS-FASL interactions are deficient. The first, generalized lymphoproliferative disease (*gld*) mice have a spontaneous germline mutation in *FASL* that causes a decreased binding affinity between FASL and FAS and leads to lymphadenopathy and autoimmunity[107]. The second is the lymphoproliferation (*lpr*) mouse model that has a spontaneous insertion in intron 2 of the *FAS* gene. As a result, *lpr* mice develop lymphadenopathy, systemic lupus erythematosus-like autoimmune disease and have an increased incidence of lymphoma[108,109]. These models have provided insight into FAS-FASL interactions and the effects of loss of function of either of these proteins. Furthermore, the increased risk of lymphoma in these two mouse models together with that in patients with ALPS, further iterates the importance of FAS-FASL signaling in tumor suppression.

3.5. *FAS* mutations in cancer

Somatic *FAS* mutations have been reported in many different human cancers. They have been described in diverse hematological malignancies including multiple myeloma, where both point mutations and loss of *FAS* expression were found[110]. In adult T cell leukemia, mutations were found to result in the loss of *FAS* expression on the cell surface[111]. In childhood T-cell acute lymphoblastic leukemia, two different *FAS* mutations were identified and were associated with resistance to apoptosis[112]. In addition, Grønback *et al*. identified *FAS* mutations in 11% of the NHL samples in their study, and found them to be associated with extranodal disease, yet functional studies were not performed to determine the impact of these reported mutations[113]. Most recently, Pasqualucci *et al*. reported that *FAS* mutations were present in 10% of TLy, and concluded that they may be associated with FL histologic transformation[30]. *FAS* mutations have also been reported in non-hematological malignancies including bladder cancer, where 28% of tumors analyzed were positive for *FAS* mutations, including missense and frameshift mutations[114]. *FAS* mutations were also found in other solid tumors including some gastric

cancers [115], melanomas[116] and non-small cell lung cancers[117]. Although *FAS* mutations have also been reported in lymphoma and other malignancies, they have not been studied in the context of therapeutic resistance in FL.

Chapter 2: The role of FAS in lymphoma

2.1. Introduction and Rationale

In spite of improvements in the development of treatments for NHL, therapeutic resistance remains the main cause of mortality in a subset of patients with primary treatment failure. Recent sequencing efforts have identified genomic alterations in FL and DLBCL[30,118-120]. Yet, the challenge remains to identify which are clinically relevant and contribute to the development of therapeutic resistance and aggressive disease[19]. To address this problem, we previously analyzed the transcriptomes of biopsies from FL patients before and after therapy to identify target gene mutations enriched for in tumors at relapse. *FAS* mutations have been reported by Pasqualucci et al, to occur in 10% of TLy [30], however, most patient with TLy in this study were exposed to chemotherapy and therefore it is difficult to determine if the *FAS* mutation occurred under the selection pressure of chemotherapy or at histological transformation.

In a cohort of 214 previously untreated FL, we previously found *FAS* mutations to be uncommon at diagnosis (3%; 6/214) yet common at relapse, where 11 of the 214 patients in this cohort developed chemotherapy-refractory disease and of these, 27% (3/11) had *FAS* mutations. Furthermore, *FAS* mutations in FL were associated with an earlier time to progression (only 1 year vs 2.8 years, $p>0.05$) and an increased risk of histological transformation to DLBCL (n=4/6, $p<0.05$) (unpublished data). Furthermore, in a recent clinical trial at our institute, (QCROC2) 15% of rrDLBCL had mutations in *FAS* (unpublished data). This led to the identification of FAS as a potential tumor suppressor important in FL and DLBCL disease progression and resistance to standard chemotherapies. *FAS* mutations are apparently clinically relevant, and it is therefore critical to study their role in contributing to therapeutic resistance in lymphoma.

For preliminary *in vitro* work, our lab focused on a hot spot Y232* mutation (leading to a stop codon replacing tyrosine residue 232) that predicted for a truncated protein lacking a functional death domain. We previously found that upon stimulating FAS signaling with the FAS agonistic antibody, CH-11 (a FASL mimic), as expected, based on similar studies shown in ALPS, cell

lines transfected with *FAS*(Y232*) resulted in defective extrinsic apoptosis, in comparison to cells transfected with either *FAS* WT or the vector alone[106]. However, when we treated these same cells with chemotherapy *in vitro*, the *FAS*(Y232*) mutation did not confer resistance. This finding was not surprising, due to the fact that FAS depends on activation by its cognate ligand FASL, absent from *in vitro* cultures. This coupled with recent evidence that CD8+ T cells control the development of spontaneous B cell lymphoma in a FAS-FASL dependent manner[83], necessitated that we develop an *in vivo* model of *FAS*-mutant lymphoma to more appropriately determine the effects of this mutation on tumor growth and response to chemotherapy, and to better understand the interactions between FAS and FASL in the lymphoma microenvironment.

Hypothesis

We hypothesize that *FAS* mutations evade the FAS-FASL-mediated immune response leading to increased tumor size and resistance to conventional therapy.

Objective

The overall objective is to better understand the role of *FAS* mutations and FAS-FASL interactions in lymphoma, in order to ultimately target *FAS*-mutant lymphomas.

Specific aims

1) Develop an immunocompetent *in vivo* model of Fas-mutant lymphoma with the E*u-Myc* cell line ($ARF^{-/-}$).
2) Test whether Fas mutations affect lymphoma growth and response to chemotherapy in immune competent mice.
3) Confirm that Fas mutant lymphomas must be studied in an immunocompetent model, using immunodeficient mice (SCID and SCID beige mice) as E*u-Myc* lymphoma recipients.
4) Test whether doxorubicin and cyclophosphamide (components of R-CHOP) affect the expression of *Fas* and *Fasl* on cells of the lymphoma microenvironment in our model.

5) Determine the effects of doxorubicin and cyclophosphamide on the expression of *FAS* in 4 novel human NHL cell lines (DLBCL and Burkitt lymphoma).
6) Determine the outcome of patients with *FAS*-mutant rrDLBCL and TLy.
7) Identify any genes that are differentially expressed between *FAS*-mutant and *FAS*-WT lymphomas.

2.2. Methodology

Cell lines and culture

E*μ-Myc* ($Arf^{-/-}$) murine B cell lymphomas were a kind gift from Dr. Scott Lowe (Memorial Sloan Kettering Cancer Center)[121,122] and were cultured in B cell medium (45% Dulbecco's Modified Eagle Medium (DMEM), 45% Iscove's Modified Dulbecco's Medium (IM-DMEM), 10% Fetal Bovine Serum (FBS), 0.55 mM β-mercaptoethanol , 5% L-glutamine and 5% Penicillin and 5% Streptomycin), on a monolayer of gamma-irradiated *Ink4a*$^{-/-}$ murine embryonic fibroblasts (MEF) (gift from Dr. Jerry Pelletier), as feeder cells. MEFs were gamma-irradiated as previously described[123] to mitotically inactivate them preventing the dilution of E*μ-Myc* cells with dividing fibroblasts. Irradiated MEFs are suitable as a feeder layer, as not only do they provide sufficient nutrients, but unlike E*μ-Myc* cells, MEFs are adherent cells[123]. 293T cells used to generate retroviral stocks were grown in DMEM supplemented with 10% FBS (and 5% Pen/Strep and 5% L-glutamine).

4 novel patient cell lines (for the purpose of this thesis named Cell line 1, 2, 3 and 4) that were previously developed in our lab from primary patient lymphoma cells obtained from lymphoma division of the "Quebec Leukemia Cell Bank" at the Jewish General Hospital. Patients consented to participate in this research project and the use of these patient samples was approved by the Jewish General Hospital Research Ethics Board. The samples were obtained from either biopsy or blood from patients at either the time of diagnosis or progression. Patient treatments were not altered because of this research. Patient Cell lines 2, 3, 4 were infected with EBV for immortalization. Cell lines 1 and 2 were developed from samples from patients with DLBCL, and Cell lines 3 and 4 were developed from patients with Burkitt's lymphoma. Cell line 1 is known to have a *FAS* mutation, and is p53 WT (part of the clinical trial NCT01238692). Cell line 2 is known to be *FAS* WT and have a p53 mutation. Cell line 3 is known to have a p53 mutation and to be *FAS* WT, finally Cell line 4 is *FAS* WT and p53 WT. Patient Cell lines were maintained in Roswell Park Memorial Institute medium 1640 (RPMI medium) (supplemented with 20% FBS, 5% L-Glutamine and 5% Pen/Strep).

BJAB human lymphoma cell lines were grown in RPMI 1640 supplemented with 10% (FBS; Wisent), 5% streptomycin and 5% penicillin (Pen/Strep). The selection agent G418 was added to the cultures at a final concentration of 0.8 mg/ml for the BJAB stable transfectants. All the cells were maintained at 37°C in a humidified incubator with 5% CO_2.

Generation of BJAB *FAS* mutants and control cell lines

The *FAS*(Y232*) mutant coding sequence, which lacks the last c-terminal 104 amino acids of *FAS*WT, was generated by PCR using the oligos "FlagFAS HindIII" Sense 5'-AAG AAG CTT ACC ATG CTG GGC ATC TGG ACC CTC CTA CCT CTG GTT CTT ACG TCT GTT GCT AGA TTA TCG TCC AAA GAC TAC AAG GAC GAC GAT GAC AAG AGT GTT AAT GCC CAA GTG-3' and "FASDD XhoI antisense" 5'- CGCG CTC GAG TTA TTT ACT CAA GTC AAC ATC-3', and *FAS* cDNA as template. Similarly, the wild-type coding sequence was amplified with the oligos "FlagFAS HindIII sense" and "FASWT XhoI antisense" 5'-GGC CTC GAG CTA GAC CAA GCT CTG GAT TTC-3'. These sequences were then inserted into pcDNA3.1 to yield the constructs pcDNA3.1-FlagFASDD and pcDNA3.1-FlagFASWT. Both *FAS* inserts were sequenced to ensure that no mutations were introduced during the PCR procedures.

Transfected cells were selected with G418 and purified using a BD FACS Vantage SE cell sorter, by only collecting cells that stained with anti-FAS PE (Becton Dickinson, BD), clone 15A7 is reported by manufacturer to not induce apoptosis in Fas-expressing cells. These were cloned by limiting dilution, and clones that showed similar levels of exogenous FAS were expanded and used for the nanostring gene expression profiling experiment.

Generation of Eμ-*Myc* Fas mutant and control cells

The murine equivalent of the *FAS*(Y232*) truncating mutation, Fas(Y224*) (or FasDD) and murine FasWT (to overexpress full length wildtype Fas) inserted into the retroviral vector pMIG (MSCV-IRES-GFP) (Addgene). The mutant Fas coding sequence was amplified from *Fas* cDNA with the oligos "Fas EcoRI sense" 5'- CTG GAA TTC GCT GCA GAC ATG CTG TGG ATC

TGG GCT G -3' and "FasDD XhoI antisense" 5'- GGG CTC GAG CTC GGG ATC TAT TTA CTC AAG C -3'. Likewise, the wild-type Fas coding sequence was amplified using the oligos "Fas EcoRI sense" and "FasWT EcoRI antisense" 5'- GGC GAA TTC TCA CTC CAG ACA TTG TCC TTC -3'. Following restriction digestion, these products were inserted into the retroviral vector MSCV-IRES-GFP, to yield MSCV-FasDD-IRES-GFP and MSCV-FasWT-IRES-GFP, respectively. The inserts were sequenced to verify their integrity and proper orientation in the vector. This vector allows for the production of retroviral particles that express a gene of interest under the Murine Stem Cell Virus (MSCV) promoter and green fluorescent protein (GFP) on the same messenger RNA, separated by an internal ribosomal entry site (IRES). 293T cells were transfected with the two Fas retroviral constructs or the control empty vector and the pCL-ECO retrovirus packaging vector (Addgene) using jetPRIME reagent (Polyplus transfection). Two days later, their supernatants, containing Fas-expressing retrovirus, were used to infect E*μ-Myc* cells, in the presence of polybrene (4 μg/ml; Sigma), as it has been shown to increase gene-transfer efficiency by increasing viral absorption in target cell membranes [124]. The infected cells were then stained with anti-FAS PE (BD) antibody, that does not induce apoptosis in Fas-expressing E*μ-Myc* cells, and strong double GFP-positive and FAS-positive cells that would indicate high of exogenous FAS protein [either Fas WT or Fas(Y224*)] were sorted by cytometry and allowed to grow for 48 hours on iMEFs in order to provide cells time to recover and have enough cells to inject 1 million cells per mouse (n=10 mice per group). Vector control E*μ-Myc* cells were prepared in the same way, however single GFP+ cells were sorted by cytometry, where GFP indicates the expression of the vector, and in this case, there is no expression of exogenous Fas. E*μ-Myc* cells (Fas(Y224*), FasWT, VC and non-transduced as negative controls) were stained with BV421-conjugated anti-mouse FAS antibody (BD) at 4°C for 30 minutes in the presence of 4% FBS washed and then analyzed by flow cytometry using the BD LSRFortessa™ cell analyzer for both GFP and FAS expression (Figure 2.1 A).

In vitro E*μ-Myc* experiments

In order to determine the growth characteristic of E*μ-Mycs* with the different Fas genotypes, $0.5x10^6$ lymphoma cells were grown on iMEF feeding monolayers. At each time point GFP-

expressing cells (E*μ-Myc* cells of different Fas genotypes) were counted using a flow cytometer at 0, 24, 48, 72 and 96 hours.

The response of E*μ-Myc* with different Fa*s* genotypes to doxorubicin (Selleckchem) *in vitro* was determined by incubating $1x10^6$ cells with different concentrations of doxorubicin, for 12 hours. Cells were then stained with Near-Infrared Live/Dead fixable dead cell stain (Invitrogen) and the percentage of live E*u-Myc* cells (GFP-expressing cells) was determined for each sample by flow cytometry BD LSRFortessa™ cell analyzer.

In vivo E*μ-Myc* experiment

$1x10^6$ E*μ-Myc* cells of each Fas genotype (Fas(Y224*) mutant, FasWT or vector control) were injected into the tail vein of C56BL/6 mice (8 week old females; 10-13 per group, Charles River Laboratories). On day 11, the mice were injected intraperitoneally with doxorubicin (10 mg/kg). Lymphoma progression and response to treatment was monitored using 3-dimensional-ultrasound Vevo770 system (Visualsonics) of both inguinal lymph nodes on days 0, 8, 11, 12, 13, 15 and 18 post-inoculation.

This experiment was then repeated in SCID (lack mature and functional B and T cells)[125] and SCID beige (lack functional B, T and Natural killer cells)[126] mice in order to determine whether a functional immune system is required for the Fas mutant lymphoma aggressive phenotype, with C57Bl/6 as controls. In all experiments mice were sacrificed at individual humane sacrifice points using Body Condition Score (BCS) less than 2 or apparent paralysis, as endpoints. Animal studies were approved by McGill University's Animal Resource Centre and complied with the guidelines set by the Canadian Council of Animal Care.

Fas/Fasl expression in cells of the microenvironment

In order to determine the effects of doxorubicin and cyclophosphamide (Jewish General Hospital oncology-department pharmacy) on *Fas* and *Fasl* expression in cells of the tumor microenvironment a different time points post-treatment, $1x10^6$ GFP expressing E*μ-Myc* cells

(vector controls) were injected into the tail vein of C56Bl/6 mice (8 week old females; 4 mice per group). On day 7 after cell injection, the mice were treated by intraperitoneal injection with either doxorubicin (10 mg/kg) or cyclophosphamide (150mg/kg). Mice were anesthetized with isofluorane then euthanized with CO_2 and cervical dislocation at either 6, 24 or 48 hours post-treatment. Injection of lymphoma cells and treatments for each group were scheduled on consecutive days such that all mice would be treated 7 days after cell injection, and that all mice would be euthanized on the same final day. A non-lymphoma control group was included, as well as the appropriate no treatment controls. Once mice were euthanized, inguinal lymph nodes were collected and cell suspensions were made. 1 million cells from each cell suspension were stained with near-infrared LIVE/DEAD (Invitrogen) for 30 mins, blocked with 20% FBS and then stained with a panel of fluorochrome-conjugated antibodies, in the presence of 2% FBS, [CD3-AF700; CD4-V500; CD8- PE-CF594; CD19-AF647; FAS-BV421; and FASL-PE; (BD)] each pre-titrated using the method described by Hulspas [127]. This multicolor panel was designed based on the following approach described by Baumgarth and Roederer [128]. Fluorescence Minus One (FMO) controls and Single Stained (SS) controls were included as previously described [129]. *Fas* and *FasL* expression (Mean Fluorescence Intensity (MFI)) on live cells of the immune system (CD8+ T cells, CD4+ T cells, CD19+ non-malignant B cells and CD19+ GFP+ malignant B cells) between non-treated controls and cyclophosphamide or doxorubicin treated groups at either 6, 24, 48 hours post-treatment, were compared.

FAS expression in novel human lymphoma cell lines after chemotherapy

In order to determine the effect of chemotherapy on the expression of *FAS* in human lymphoma cell lines, 6 x 10^5 cells of each of patient cell lines 1, 2, 3, and 4 were cultured. Cells were then treated with three doses of doxorubicin and three doses of etoposide (Jewish General Hospital oncology-department pharmacy), for 24 hours, each in triplicate. Appropriate non-treated control cells were used. Cells were harvested after 24 hours and stained with both near-infrared Live/Dead stain (Invitrogen) for 30 mins (in the absence of FBS), blocked with 20% FBS and then stained with PE-conjugated anti-human FAS antibody (BD) in the presence of 2% FBS. Both the Live/Dead and FAS antibodies were pre-titrated using the method described by Hulspas[127]. As for the E*μ-Myc* cells, the multicolor panel was designed based on the following

approach described by Baumgarth and Roederer[128]. FMO controls, SS controls (including a doxorubicin only treated control) were also included as part of the flow analysis, and compensation was performed as previously described[129]. *FAS* expression was analyzed with the BD LSRFortessa™ cell analyzer and FlowJo software (Tree Star Inc., Ashland, OR) normalized to live cells and presented as relative to the non-treated controls.

Relapsed or refractory DLBCL patients

The cohort consisted of 33 patients with rrDLBCL that were obtained after at least one cycle of immunochemotherapy, of which 25 evolved from *de novo* DLBCL and 8 were TLy. Samples were obtained prospectively from patients enrolled in the QCROC-2 clinical trial NCT01238692. This study was approved by the Jewish General Hospital Research Ethics Board.

RNA and DNA isolation

Three needle core biopsies were pooled in RPMI media, disaggregated in a cell suspension and purified for B cells that were selected using a magnetic bead negative selection technique (human B-cell enrichment cocktail without CD43; Stem cell technologies) as previously described [130]. DNA and RNA from purified B cells were isolated using the AllPrep kit (QIAGEN).

Gene expression profiling and gene set enrichment analysis

We investigated the gene expression profiles (GEP) of *FAS*-mutant lymphomas using two complementary approaches. First, total RNA isolated from the purified lymphoma cells was used in cDNA microarray analyses using either the Sureprint 8 x 60K one-color human expression array (Agilent) or the Human Gene 2.0 ST array (Affymetrix) platforms. The COO (LLMP score) was calculated using the subgroup of predictor genes identified by Wright et al., [131]. A list of top 100 upregulated and down-regulated genes in *FAS*-mutants was generated. Our dataset representing genes with altered expression profile in *FAS*-mutant lymphomas derived from array

analyses were imported into the Ingenuity Pathway Analysis Tool (IPA Tool; QIAGEN Silicon Valley) that allows for the identification of biological networks, global functions and functional pathways of a particular dataset. Secondly, targeted GEP was performed using the nanoString nCounter gene expression system (nanoString Technologies)[132] using an apoptosis nCounter Gene Expression codeset containing a panel of 162 immune-related genes (See Supplemental Table 1 for specific genes). Samples were hybridized in biological triplicates using 140 ng total RNA per reaction according to the manufacturer's instructions. All data analyses were performed using the nSolver Analysis Software version 2.5 (nanoString Technologies). Background hybridization was determined using spiked-in negative controls. All signals below mean background plus 2 standard deviations were considered to be below the limits of detection. Raw counts above background were normalized using the mean of the spiked in exogenous positive controls. Then, a content normalization factor was calculated from the geometric mean of the reference genes and applied to the data previously normalized by the positive control.

We then performed GEP on our BJAB cell lines. RNA was extracted using BJAB cells transfected with the three *FAS* genotypes before and after a six-hour exposure to 500ng/ml CH-11 antibody (Beckman Coulter), using the All-Prep RNA/DNA kit (Qiagen). Detection of mRNA transcripts was then carried out in multiplexed hybridization reactions using the NanoString nCounter Analysis System using the same apoptosis nCounter Gene Expression CodeSets as the patient primary samples. Data acquisition, normalization and analysis were carried out as with the patient samples nanostring experiment. Finally, we validated this gene list in our primary rrDLBCL samples with the results from our cell lines using Gene Set Enrichment Analysis (GSEA)[133,134].

Statistics

All statistical analyses were performed using a two-tailed Student t test. With the exception of the E*μ-Myc* proliferation and doxorubicin cytotoxicity assays, curves were compared using a 1-way ANOVA. P values <0.05 were considered statistically significant. Statistical analyses were performed using SPSS software version 11.0 and R version 2.7.2. All graphs were created using the GraphPad Prism software version 6.0 for Mac (La Jolla, CA, USA).

2.3. Results

Fas(Y224*) does not affect lymphoma growth or response to doxorubicin in E*μ-Myc* lymphoma cell line *in vitro*.

Considering our previous findings (unpublished data) that the *FAS* mutation does not cause cells to be inherently resistant to chemotherapy *in vitro*, we hypothesized that immune and/or stromal factors present in patient lymph nodes, such as FASL present on cytotoxic T lymphocytes, are responsible for the aggressive clinical behavior of *FAS* mutant lymphomas. In order to address whether *FAS* mutations can accelerate growth and induce resistance to chemotherapy *in vivo*, we used the well-characterized immunocompetent E*μ-Myc* mouse lymphoma model[36,37,135-137]. We infected an E*μ-Myc* murine cell line with either the murine equivalent of human *FAS*(Y232*), Fas(Y224*), murine FasWT, or empty vector control, and confirmed expression of our vectors by FCM, using the expression of FAS and GFP as readouts (Figure 2.1A). We then wanted to determine whether the Fas mutation had an effect on growth characteristics and sensitivity to chemotherapy *in vitro* in this murine cell line. We found no differences in the number of live cells between the three E*μ-Myc* groups throughout a 4-day growth experiment ($p>0.05$) (Figure 2.1B). Furthermore, as we previously observed in human cell lines, there was no difference in chemo-sensitivity upon exposure to doxorubicin in these cells when cultured on iMEF support cells (Figure 2.1C). The three curves are not significantly different ($p>0.05$).

The Fas genotype modulates lymphoma growth and response to chemotherapy in immunocompetent mice

Because we think that the host-tumor interaction might be necessary to promote growth and resistance to chemotherapies in the presence of a *FAS* mutation, we next utilized the well-characterized *in vivo* E*μ-Myc* mouse lymphoma model to test our hypothesis[36,135,138]. We transduced an E*μ-Myc* murine cell line with either the murine equivalent of human *FAS*(Y232*), Fas(Y224*), murine FasWT, or empty vector control. We then injected three groups of immunocompetent mice with these lymphoma cell lines that differed only in their Fas genotype. and monitored lymph node volumes before and after doxorubicin treatment. The vector control

group developed lymphadenopathy by day 8, were treated with doxorubicin on day 11 and lymphadenopathy resolved by day 15 (Figure 2.2A). Fas(Y224*) mutant lymphomas grew more rapidly in comparison to controls and tumor volumes exceeded those measured in FasWT and vector control mice at all time points beyond the day of injection ($p<0.05$).

The average maximal lymph node volume for the Fas(Y224*) group was 59.9 mm^3 compared to 18.9 mm^3 and 34.5 mm^3 for the FasWT and control groups, respectively ($p<0.001$). Furthermore, Fas mutant lymphomas had a delayed response to doxorubicin. None of the mice in this group achieved a complete remission, and tumor re-growth occurred earlier in comparison to controls. Mice with larger tumor volumes needed to be euthanized due to progressive disease and humane endpoint achieval, and none of these mice survived beyond day 18. The addition of FasWT resulted in a decreased tumor growth in comparison to the Fas(Y224*) mutant and in a more rapid resolution of lymphadenopathy after doxorubicin compared to vector controls. These results suggest that the presence of functional immune system may be critical for the development of the aggressive phenotype of Fas-mutant lymphomas, and that the immune response may not only control lymphoma growth but may also actively participate in chemotherapy-induced cell death.

The Fas genotype does not modulate lymphoma growth in immunodeficient mice.

We hypothesized that the increased growth *in vivo* is dependent on the presence of a functional immune system. In order to address this, E*μ-Myc* murine cells expressing either the Fas(Y224*) mutant, or the empty vector control were injected into SCID and SCID beige mice, since SCID mice lack mature T and B lymphocyte populations[125] and SCID beige additionally lack NK cells[126]. C57Bl/6 mice were injected with both cell types as controls. As expected, disease progression in the Fas-mutant lymphoma group did not differ from that of the empty vector control lymphomas when inoculated in these severely immune-compromised mice (Figures 2.3B and C), mimicking the results from our *in vitro* experiment (Figure 2.1B), where no differences in growth between the mutant and control groups were observed. However, in the C57Bl/6 mice, the difference in the size of the tumors between Fas(Y224*) and the vector control group is significant at both time points ($p<0.05$) (Figure 2.3A).

Chemotherapy modulates *Fas* and *Fasl* expression in B lymphocytes

Considering the fundamental role of the FAS pathway in immune system homeostasis and recent evidence that immune surveillance mechanisms that control the development of spontaneous B cell lymphoma rely on FAS-FASL interactions[83], we wanted to understand how *Fas* and *Fasl* expression change in cells of the lymphoma tumor microenvironment, and also after treatment with relevant chemotherapies (doxorubicin and cyclophosphamide). We injected C57Bl/6 mice with E*μ-Myc* cells that express GFP (the same vector control cells from previous experiments), allowed tumors to develop and then treated with either doxorubicin or cyclophosphamide, another component of R-CHOP recognized to have immune modulating properties[139]. Mice were then euthanized; lymph nodes were collected and made into cell suspensions at different time points after treatment. Cell suspensions were stained with a panel of antibodies to identify live cell populations, namely CD8+ T cells, CD4+ T cells, CD19+ GFP- and CD19+ GFP+, which correspond to non malignant and malignant B cells, respectively. FAS and FASL antibodies were also used in order to determine expression levels of each of the subsets of immune cells.
We first compared the expression of *Fas* and *Fasl* in cell subsets between the healthy mice and the non-treated lymphoma group (Figure 2.4A). No significant differences were found in the *Fasl* expression (as measured by MFI) in cells of the microenvironment between the healthy and lymphoma mouse groups. However, *Fas* expression was increased in the lymphoma group in CD4+ T cells, CD8+ T cells and non-malignant B cells ($p<0.05$).

We next compared the *Fas* and *Fasl* expression between the non-treated lymphoma group and the treated groups. The only group of cells to have significant time-dependent changes in *Fasl* expression after chemotherapy was the non-malignant B cells, where 24 hour post cyclophosphamide resulted in an increase in MFI from 1259 to 1536, in comparison to non-treated controls ($p<0.05$; Figure 2.4B). No other treatments resulted in significant increases in *Fasl* expression in any of the cell populations in comparison to controls (Figure 2.4B). 24 and 48 hour treatments with cyclophosphamide resulted in a significant increase in *Fas* expression in malignant B cells, where, the treatment with cyclophosphamide for 24 hours had the greatest effect increasing the MFI to 2020 in comparison to the control group with MFI of 487 ($p<0.05$). In contrast, neither of the treatments significantly increased *Fas* expression in non-malignant B

cell population in comparison to non-treated controls ($p>0.05$; Figure 2.4C), while 24 hour treatment with both cyclophosphamide and doxorubicin significantly increased *Fas* expression in both CD8+ and CD4+ T cell subsets ($p<0.05$). Finally, 48 hour cyclophosphamide also significantly increased *Fas* expression in these two T cell subsets, however, 48 hour treatment with doxorubicin did not significantly affect *Fas* expression (Figure 2.4C).

Cyclophosphamide and Doxorubicin exposure increase *FAS* expression in patient lymphoma cell lines

Considering our results from the experiment looking at *Fas* and *Fasl* expression in cells of the murine lymphoma microenvironment, where *Fas* expression was primarily effected, we wanted to confirm that *FAS* expression would be increased *in vivo* in primary patient NHL cell lines, that are well characterized in terms of *TP53* and *FAS* status, to gain insight into whether or not increases in *FAS* expression with chemotherapy rely on wild-type *TP53*. We used 4 novel human lymphoma cell lines that were recently developed in our laboratory and tested the change in *FAS* expression in each of these cell lines after 24 hour treatment with etoposide and doxorubicin. As expected all 4 Cell lines increased *FAS* expression in a dose-dependent manner. Interestingly, Cell lines 2 and 4 had a much greater relative increase in *FAS* expression in comparison to cell lines 1 and 3 at the highest dose of etoposide (Figure 2.5A and B). Cell line 2 was also found to be most sensitive to etoposide in comparison to the other three cell lines (Figure 2.5C). In contrast, Cell line 4 was not sensitive to 24 hour treatment to high doses of doxorubicin and etoposide, yet *FAS* expression was still increased in this cell line with chemotherapy treatment, regardless of p53 status.

The biology of human *FAS*-mutant rrDLBCL revealed by gene expression profiling

We compared microarray expression data from *FAS*-mutant lymphomas versus *FAS*-WT lymphomas from consenting patients that were from the Jewish General Hospital QCROC2 trial. An Ingenuity Pathway Analysis (IPA) was performed and the top molecular and cellular functions that were found to be altered between *FAS*-mutant lymphomas and the FAS-WT lymphomas were “cell death and survival” (p-values ranged: 5.77E-03 to 9.00E-12) and “cellular

compromise" (p values ranged 4.70E-03 to 9.00 E-12). IPA data is available on demand through Dr. Nathalie Johnson.

The top altered "cell death and survival gene" network was the "cytotoxicity of cells" that showed an increased activation state, with a p-value of 9.00E-12. All individual genes in this network were found to be upregulated (indicated by red colour in Figure 2.6A), namely, *TNFRSF1A, TYROBP, CASP1, CCL5, CD2, FASLG, FCER1G, FN1, GZMA, GZMB, HAVCR2, HCK, KLRB1, KLRD1, LGALS3, PLTP, PRF1 and PRKCQ*.

To validate our observations, we then decided to perform Nanostring nCounter expression analysis on these patient samples using an apoptosis CODESET, containing a panel of 162 immune-related genes, and comparing *FAS*-mutant and *FAS*-WT lymphomas. We performed a gene set enrichment analysis (GSEA) with the Broad Institute's website using gene expression data from nanostring performed on BJAB cell lines and nanostring performed on patient B cell lymphoma samples, comparing *FAS*-mutant and *FAS*-WT groups, and we identified a potential *FAS*-mutant lymphoma gene signature where the *False discovery rate* (FDR) was found to be 0.178, where the FDR $\leq$0.25 is the significance cutoff[133]. Among the genes that were found to be more highly expressed in *FAS*-mutant lymphomas are those encoding Granzyme B and CD70.

Poor clinical outcome of FAS-mutant rrDLBCL treated with HDACi

This trial revealed that 15% of rrDLBCLs have *FAS* mutations. When we compared the survival of patients with and without *FAS* mutations after treatment with HDACi, we observed that patients with *FAS*-mutant lymphomas were associated with significantly inferior survival ($p<0.001$) in comparison to the *FAS*-WT group (Figure 2.7).

A

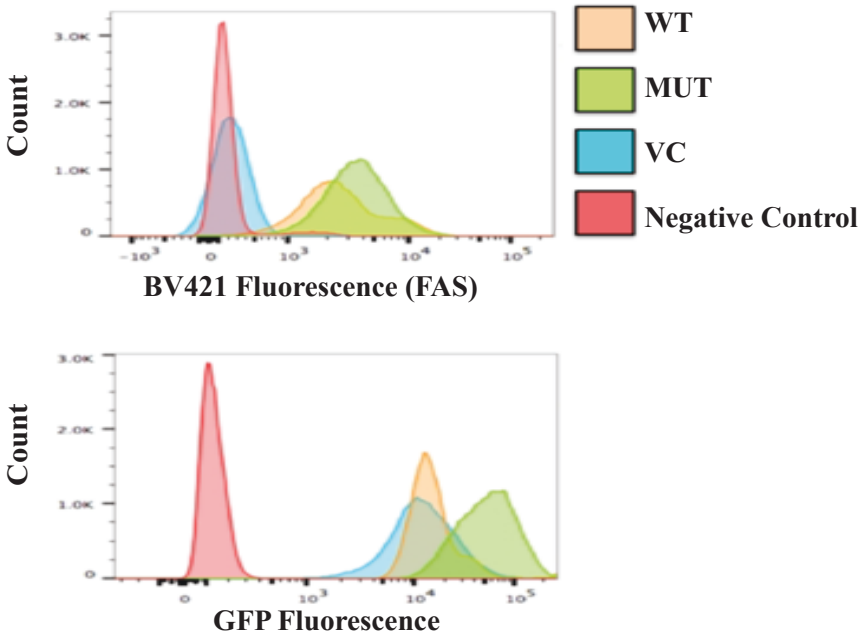
Count
BV421 Fluorescence (FAS)
WT
MUT
VC
Negative Control
Count
GFP Fluorescence

B

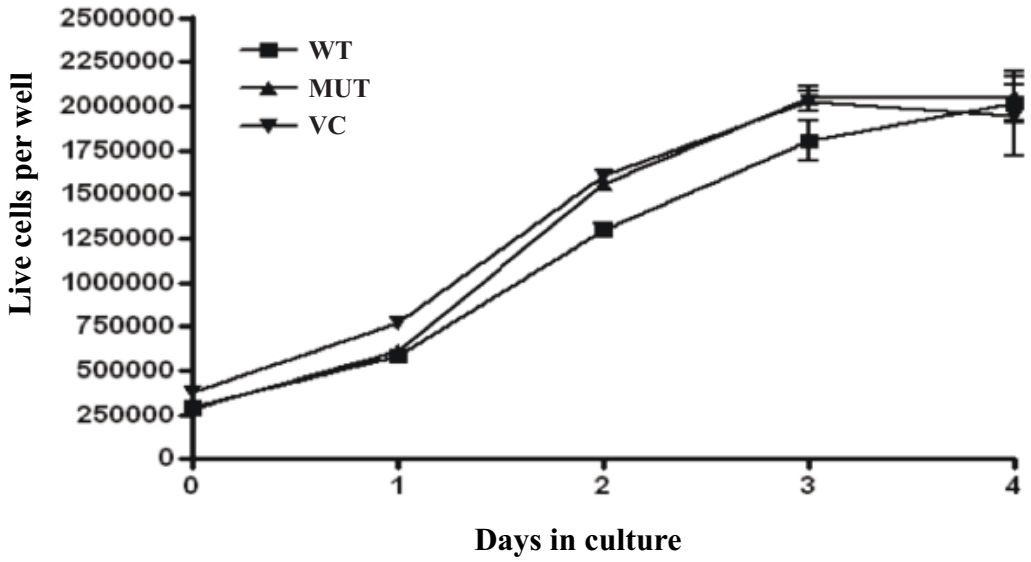
Live cells per well
WT
MUT
VC
Days in culture

C

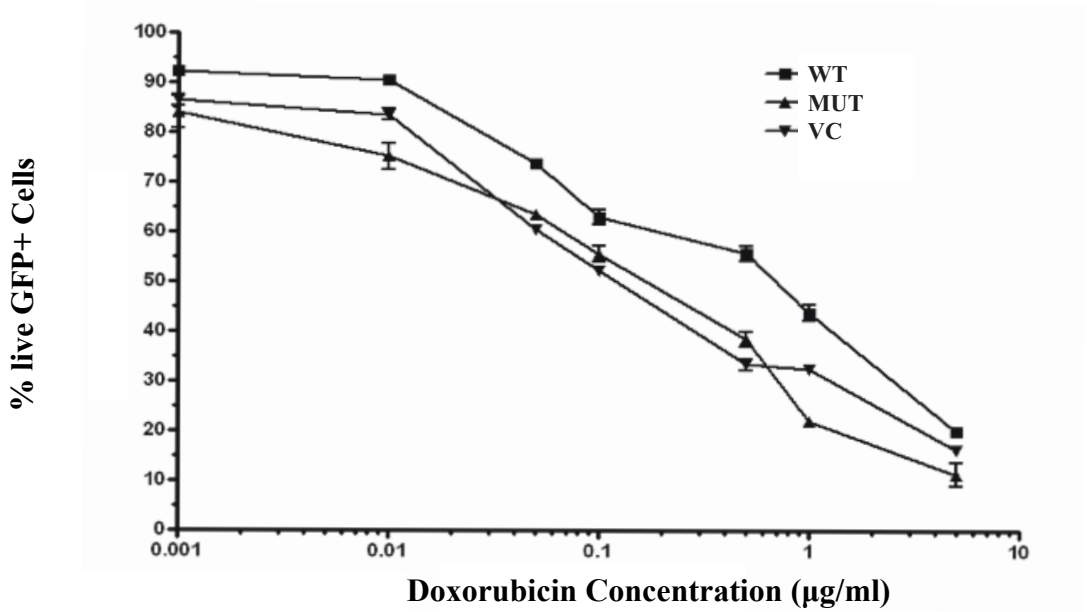
% live GFP+ Cells
WT
MUT
VC
Doxorubicin Concentration (µg/ml)

Figure 2.1. Fas genotype in murine E*μ-Myc* lymphomas does not affect total cell number or response to doxorubicin *in vitro*.
A) E*μ-Myc* lymphoma cells transduced with 3 different Fas genotypes and cultured on irradiated murine embryonic fibroblasts, were stained with BV421-conjugated anti-Fas antibody analyzed by FCM for Fas and GFP expression. B) Representation of number of live cells per well over the course of 4 days in culture. C) Cytotoxicity curve of doxorubicin on for E*μ-Myc* cells. WT: FasWT; MUT: Fas(Y224*) mutant; VC: empty vector control.

A

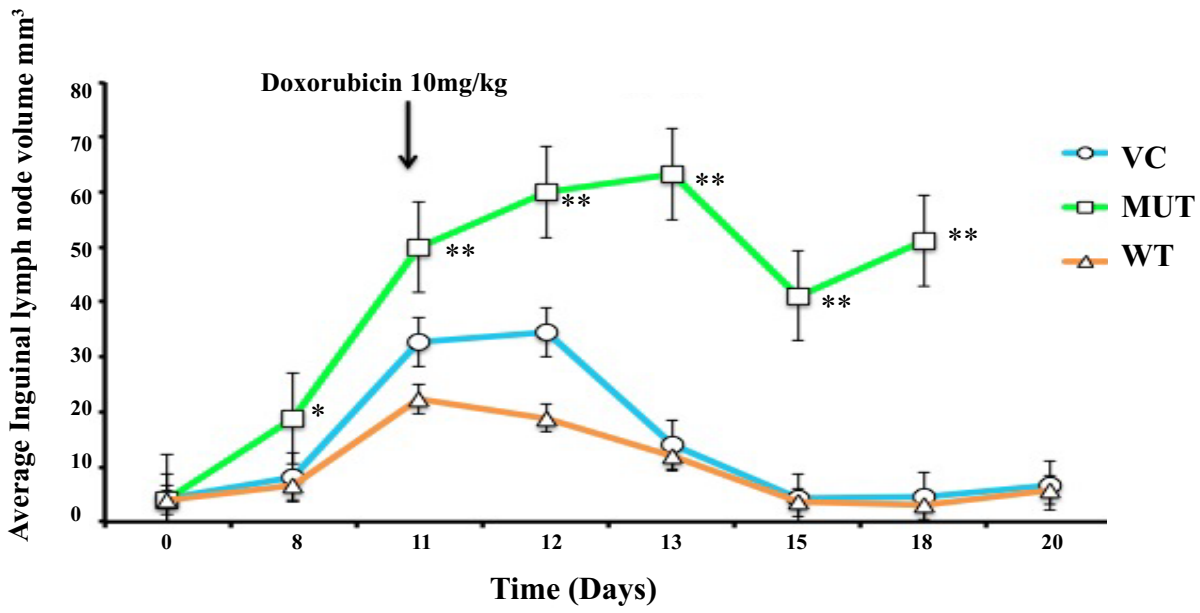

Figure 2.2. Fas genotype modulates lymphoma growth and response to chemotherapy in immunocompetent mice.

A) Lymph node volumes of mice transplanted with E*μ-Myc* lymphomas of three different Fas genotypes were measured by 3-dimentional ultrasound. Doxorubicin was administered on day 11, as indicated by arrow. WT: FasWT; MUT: Fas(Y224*) mutant; VC: empty vector controls. $p<0.05$ is indicated by * and $p<0.001$ is indicated by **.

A

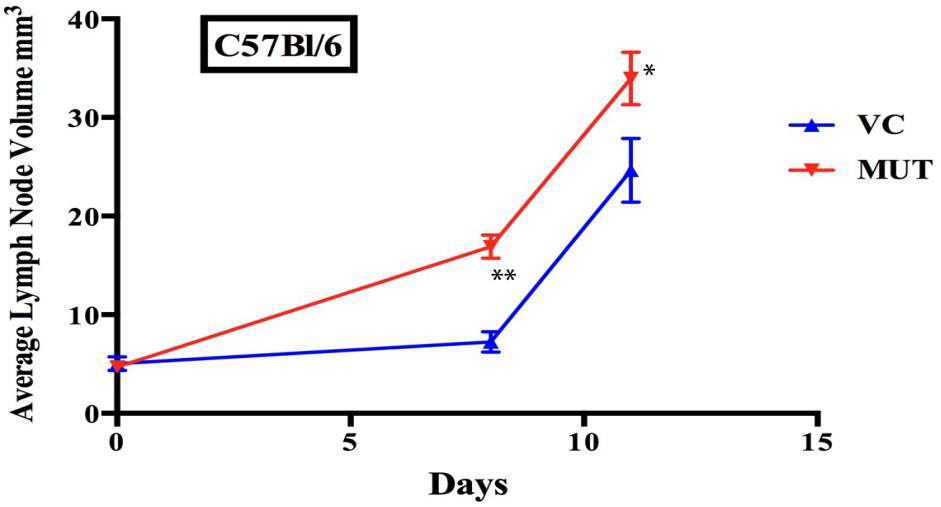
C57Bl/6
Average Lymph Node Volume mm3
40
30
20
10
0
0
5
10
15
Days
*
**
VC
MUT

B

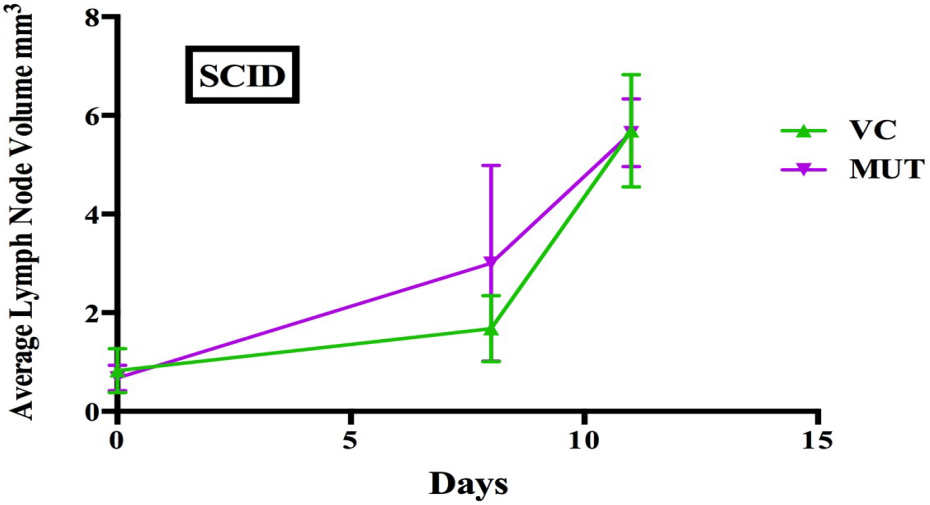
SCID
Average Lymph Node Volume mm3
8
6
4
2
0
0
5
10
15
Days
VC
MUT

C

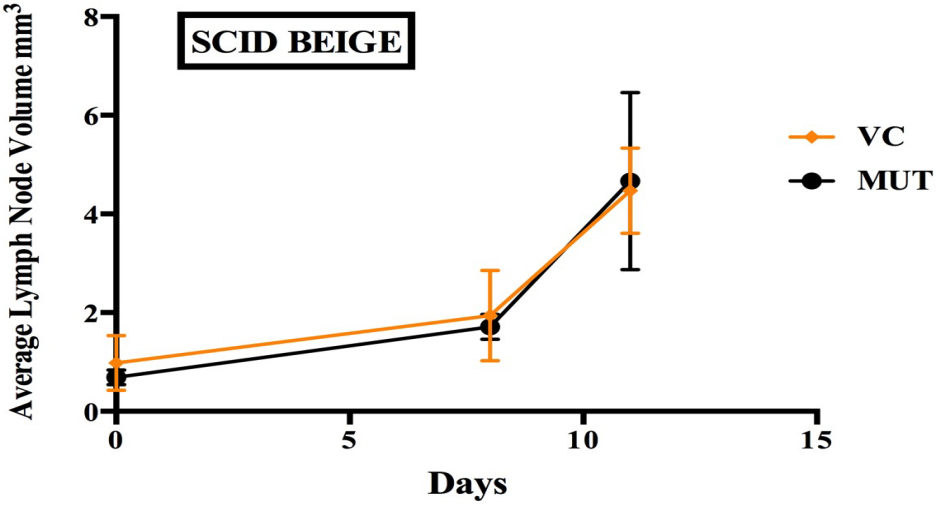
SCID BEIGE
Average Lymph Node Volume mm3
8
6
4
2
0
0
5
10
15
Days
VC
MUT

Figure 2.3. Fas genotype does not modulate lymphoma growth in immunodeficient mice. Lymph node volumes of mice transplanted with Eμ-*Myc* lymphomas of two different Fas genotypes were measured by 3-dimentional ultrasound to assess lymphoma development. In C57Bl/6 (A), SCID (B) or SCID Beige (C). MUT: Fas(Y224*) mutant; VC: empty vector controls. $p<0.05$ is indicated by *, $p<0.001$ indicated by **.

A

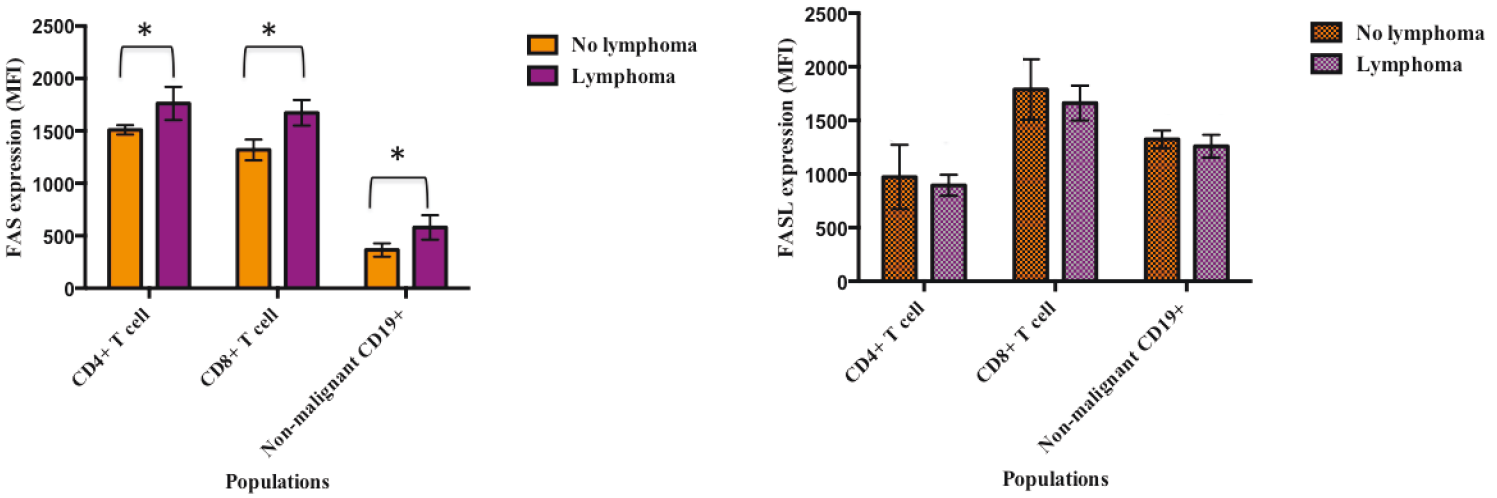
FAS expression (MFI)
2500
2000
1500
1000
500
0
*
*
*
No lymphoma
Lymphoma
CD4+ T cell
CD8+ T cell
Non-malignant CD19+
Populations
FASL expression (MFI)
2500
2000
1500
1000
500
0
No lymphoma
Lymphoma
CD4+ T cell
CD8+ T cell
Non-malignant CD19+
Populations

B

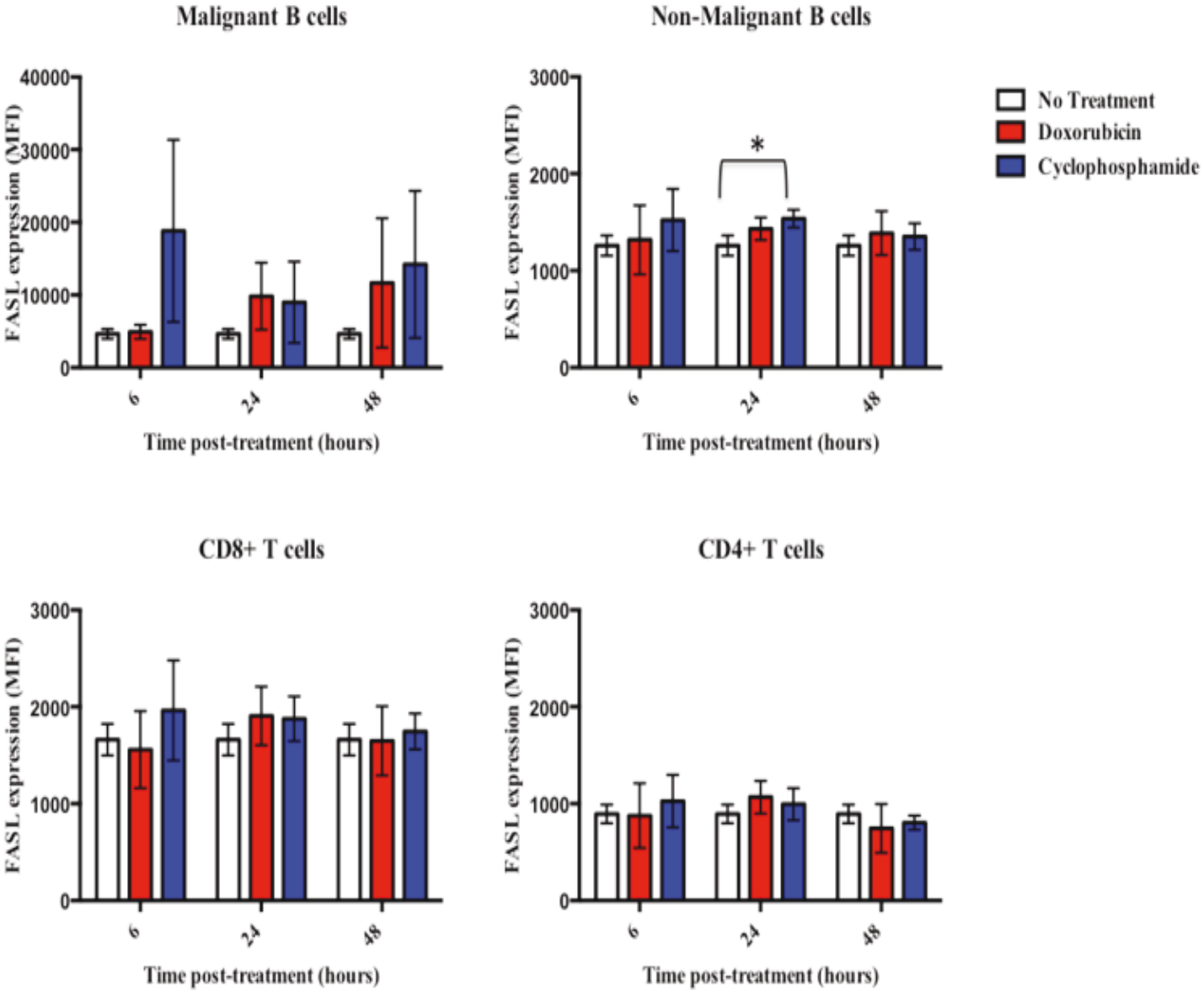
Malignant B cells
FASL expression (MFI)
40000
30000
20000
10000
0
6
24
48
Time post-treatment (hours)
Non-Malignant B cells
FASL expression (MFI)
3000
2000
1000
0
*
6
24
48
Time post-treatment (hours)
No Treatment
Doxorubicin
Cyclophosphamide
CD8+ T cells
FASL expression (MFI)
3000
2000
1000
0
6
24
48
Time post-treatment (hours)
CD4+ T cells
FASL expression (MFI)
3000
2000
1000
0
6
24
48
Time post-treatment (hours)

C

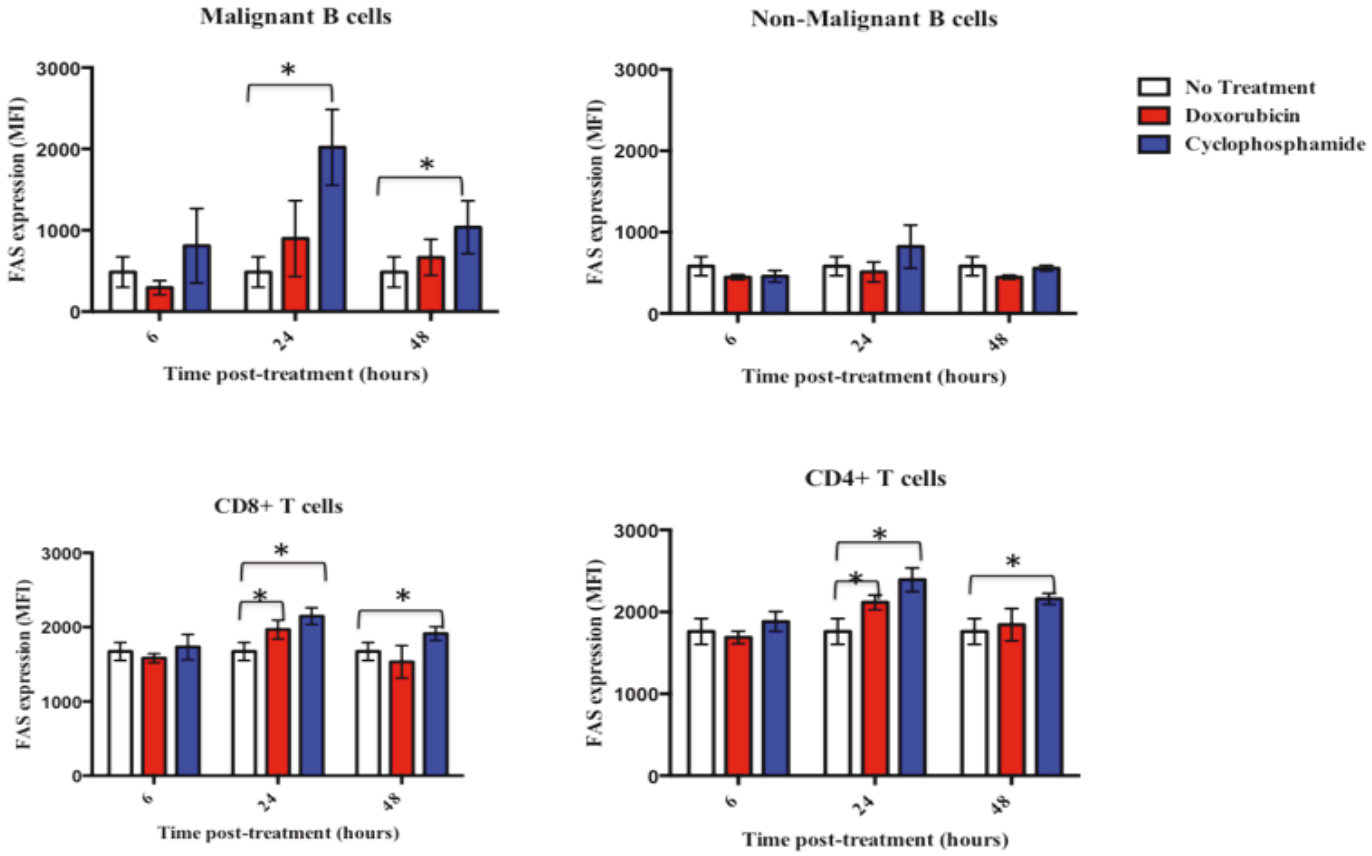

Figure 2.4. Cyclophosphamide and doxorubicin exposure increases *Fas* and *Fasl* expression in immune cells of the microenvironment to different levels.

A) *Fas* and *Fasl* expression MFI in cells of microenvironment, namely, CD8+ T cells, CD4+ T cells and non-malignant B cells, in healthy mouse controls compared to mice with E*μ-Myc* lymphoma (untreated). In B), *Fasl* and in C), *Fas* expression in different subsets of cells in the microenvironment [CD4+ T cells , CD8+ T cells, malignant B cells (E*μ-Myc* lymphoma cells) and non-malignant B cells] at different time points post-treatment with either doxorubicin or cyclophosphamide. Each treatment group is compared to their own control. * indicates $p<0.05$.

A

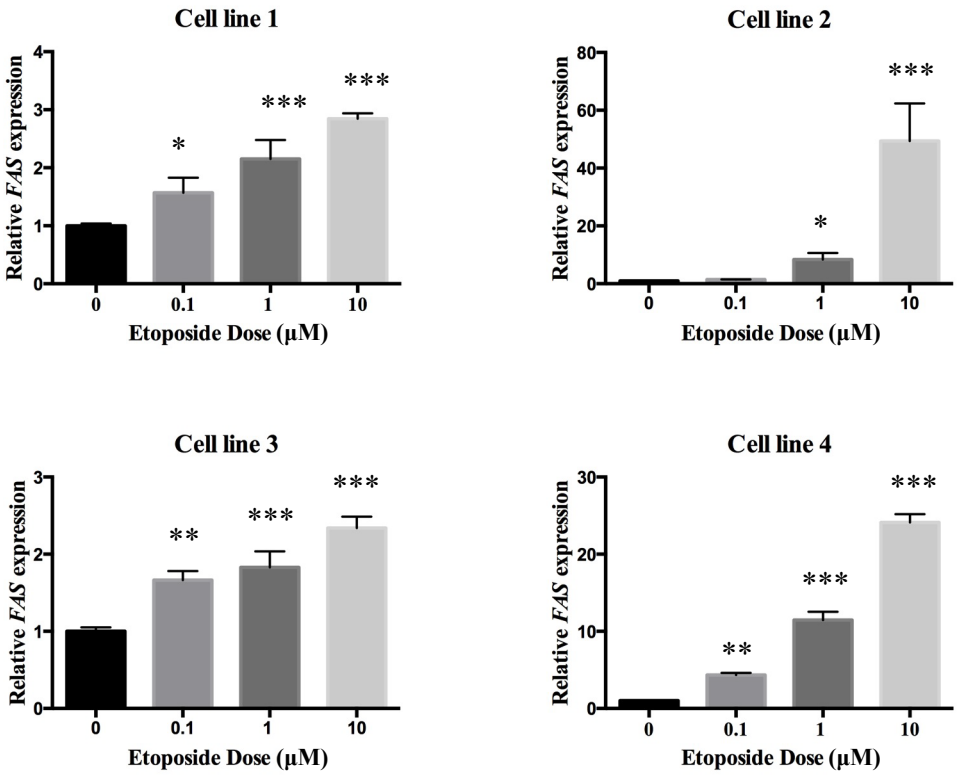
Cell line 1
Relative FAS expression
Etoposide Dose (µM)
0
0.1
1
10
*
***
***
Cell line 2
Relative FAS expression
Etoposide Dose (µM)
*
***
Cell line 3
Relative FAS expression
Etoposide Dose (µM)
**
***
***
Cell line 4
Relative FAS expression
Etoposide Dose (µM)
**
***
***

B

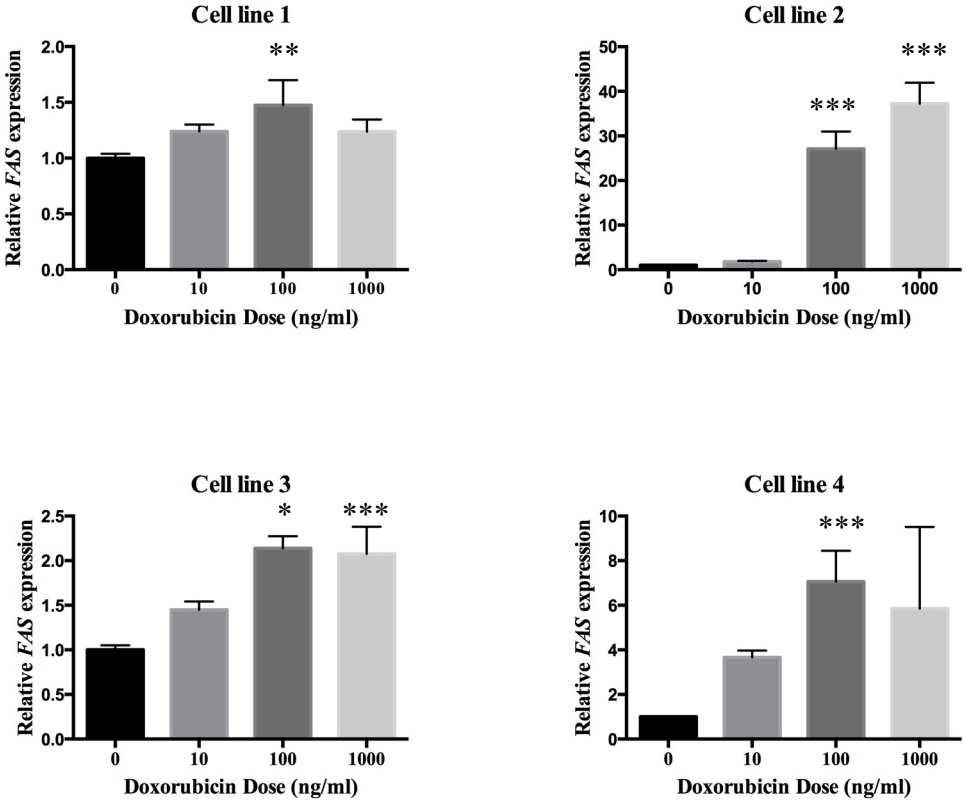
Cell line 1
Relative FAS expression
Doxorubicin Dose (ng/ml)
0
10
100
1000
**
Cell line 2
Relative FAS expression
Doxorubicin Dose (ng/ml)
***
***
Cell line 3
Relative FAS expression
Doxorubicin Dose (ng/ml)
*
***
Cell line 4
Relative FAS expression
Doxorubicin Dose (ng/ml)
***

C

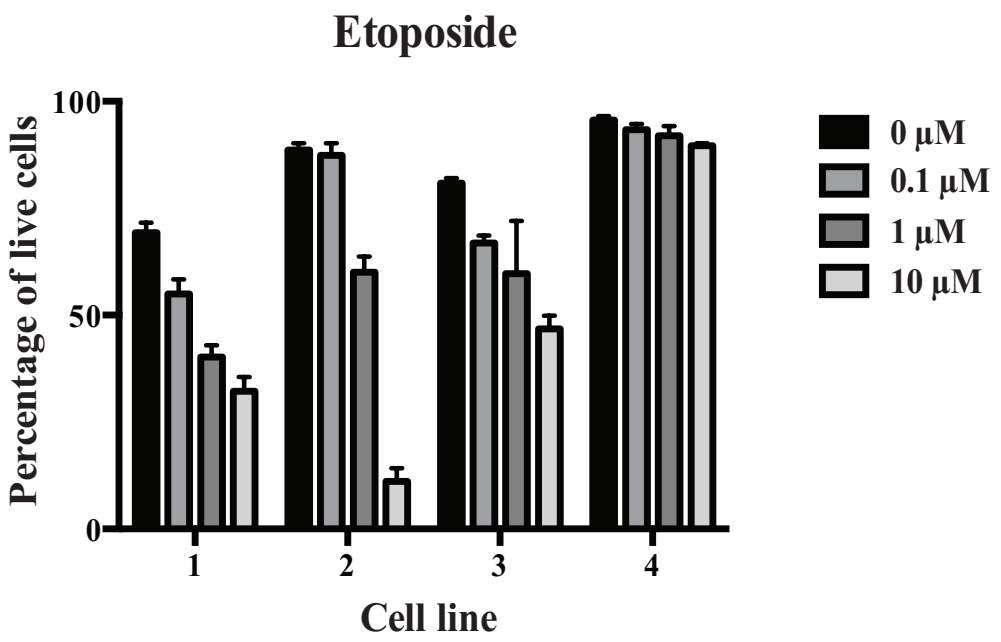

D

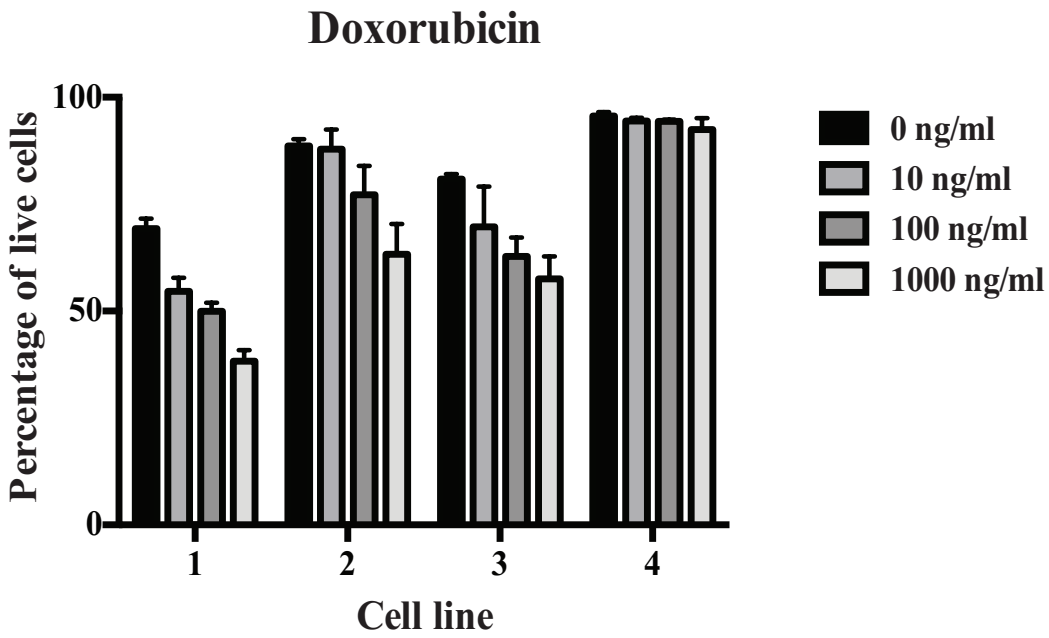

Figure 2.5. *FAS* expression is induced to different levels after treatment with chemotherapy in patient lymphoma cell lines.
Relative *FAS* expression in 4 novel patient cell lines treated with different doses of either etoposide (A) or doxorubicin (B) for 24 hours, as assessed by flow cytometry. In each case *FAS* expression was normalized to appropriate non-treated controls. C) and D) Percentage of live cells of each cell line after treatment with doses of etoposide (C) and doxorubicin (D). * indicates $p<0.05$, ** indicates $p<0.01$, *** indicates $p<0.001$.

A

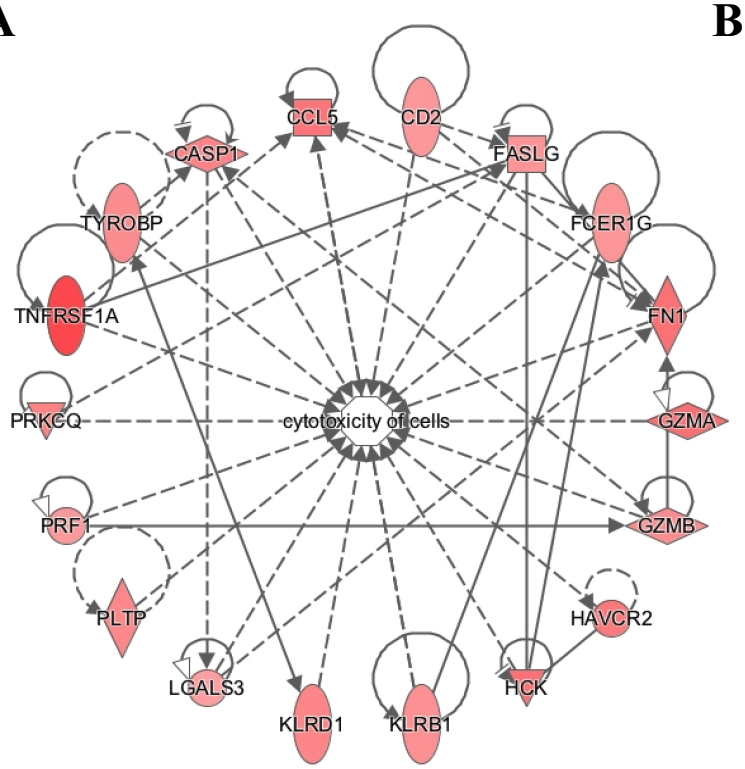
CCL5
CD2
CASP1
FASLG
TYROBP
FCER1G
TNFRSF1A
FN1
PRKCQ
cytotoxicity of cells
GZMA
PRF1
GZMB
PLTP
HAVCR2
LGALS3
HCK
KLRD1
KLRB1

B

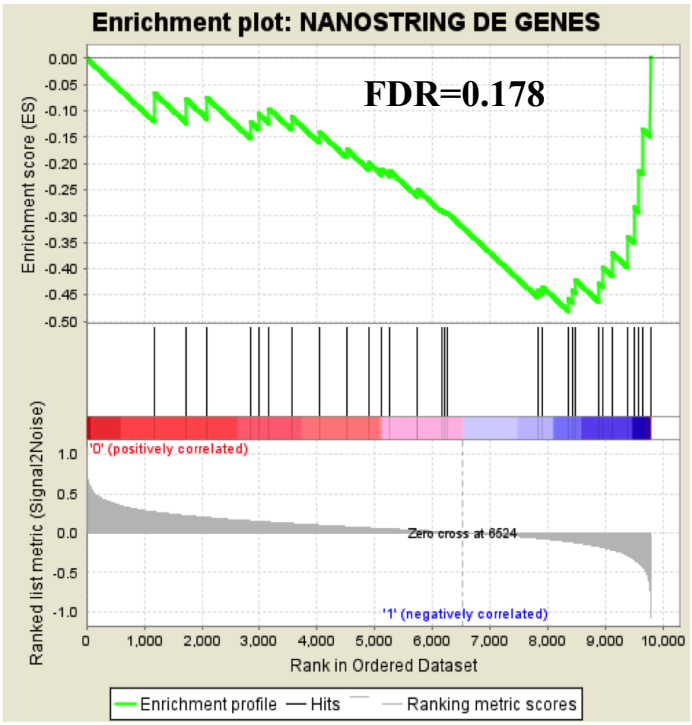
Enrichment plot: NANOSTRING DE GENES
FDR=0.178
Enrichment score (ES)
0.00
-0.05
-0.10
-0.15
-0.20
-0.25
-0.30
-0.35
-0.40
-0.45
-0.50
'0' (positively correlated)
Ranked list metric (Signal2Noise)
1.0
0.5
0.0
-0.5
-1.0
Zero cross at 6524
'1' (negatively correlated)
0
1,000
2,000
3,000
4,000
5,000
6,000
7,000
8,000
9,000
10,000
Rank in Ordered Dataset
Enrichment profile
Hits
Ranking metric scores

C

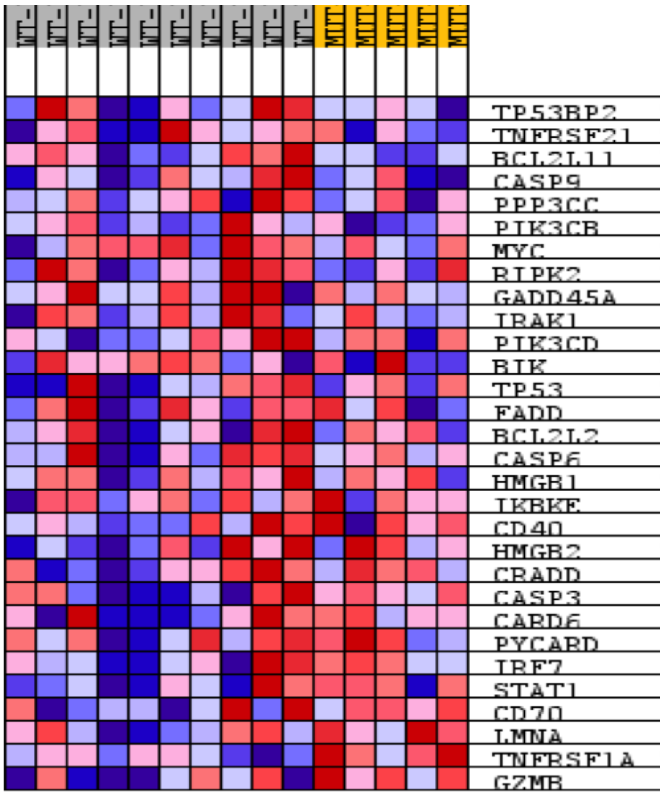
WT
MUT
TP53BP2
TNFRSF21
BCL2L11
CASP9
PPP3CC
PIK3CB
MYC
RIPK2
GADD45A
IRAK1
PIK3CD
BIK
TP53
FADD
BCL2L2
CASP6
HMGB1
IKBKE
CD40
HMGB2
CRADD
CASP3
CARD6
PYCARD
IRF7
STAT1
CD70
LMNA
TNFRSF1A
GZMB

Figure 2.6. *FAS* mutation gene signature in cell lines validates in patients.
A) Depiction of the up-regulated genes from one of the most significantly altered gene network in *FAS*-mutant lymphomas, as determined by IPA: the cytotoxicity of cells (p=9.00E-12). This was the only network where all of the genes were found to be up-regulated. A solid line represents a direct interaction between the two gene products and a dotted line means there is an indirect interaction. B) GSEA analysis comparing the signature determined from the BJAB nanostring experiment and the nanostring gene expression data obtained from comparing patient lymphoma samples with/without *FAS* mutations from the QCROC2 trial. FDR=0.178. Normalized Enrichment Score -1.33. C) Heat map of the top up-regulated and down-regulated genes in *FAS*-mutant (yellow) or *FAS*-WT patient lymphoma samples (grey) that were based on signature previously determined in BJAB cell lines. IPA: Ingenuity Pathway Analysis, GSEA: Gene Set Enrichment Analysis, FDR: False Discovery Rate.

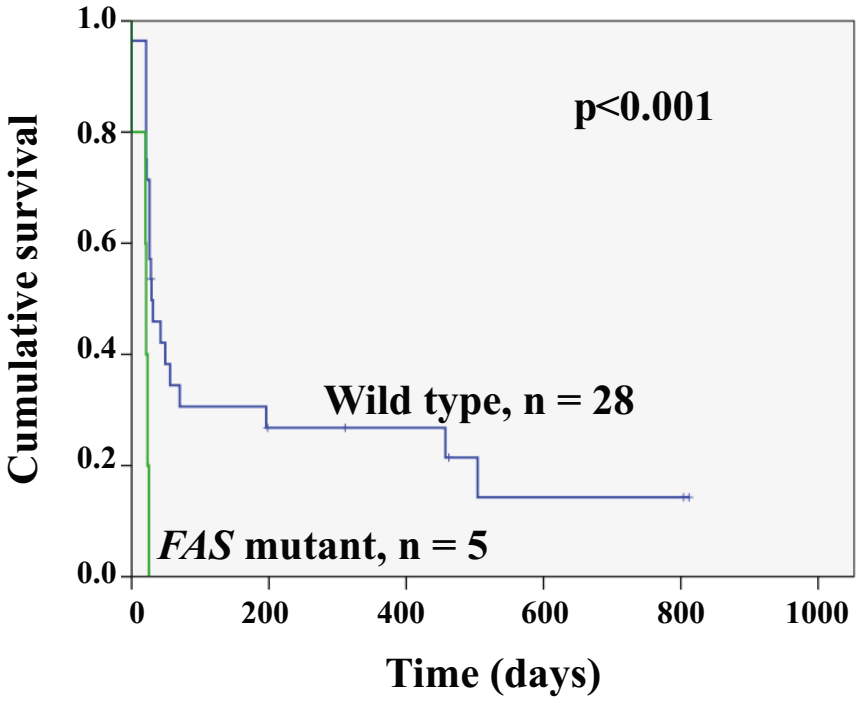

Figure 2.7. *FAS* mutations are associated with significantly inferior survival in patients with rrDLBCL.
Kaplan-Meier curve displaying the progression free survival of patients with rrDLBCL with or without *FAS* mutations, after treatment with panobinostat.

2.4. Discussion

Herein we investigated the role of *FAS* mutations in lymphoma growth and response to therapy. Initial *in vitro* experiments showed that lymphoma human cell lines infected with mutant *FAS* were sensitive to chemotherapy. Considering this, we hypothesized that immune and/or stromal factors, not present in these *in vitro* studies are responsible for the aggressive clinical behavior of *FAS*-mutant lymphomas. In order to address this *in vivo*, we first transduced the E*μ-Myc* cell line with Fas(Y224*), murine FasWT, or empty vector control. Since mutant *FAS* has been shown to have a dominant negative effect, overexpressing either Fas(Y224*) or FasWT in addition to the two endogenous FasWT alleles was appropriate for studying this mutation. Before proceeding with *in vivo* experiments, we first determined that the presence of truncated FAS protein did not have an effect on cell toxicity when exposed to chemotherapy *in vitro* in this murine cell line, as measured by cell growth. Indeed, no differences in the number of live cells between the three E*μ-Myc* groups throughout a 4-day growth experiment were observed (Figure 2.1B). To further characterize cellular response to chemotherapy, proliferation assay such as the BrdU incorporation assay for instance, will be necessary in order to provide more insight into the growth characteristics of these cells, as we cannot exclude the possibility that the proliferation of these groups of E*μ-Myc* cells differ, and may contribute to the phenotype observed in our *in vivo* experiments (Figure 2.2).

A challenge we faced was the lack of specificity of commercialized FAS antibodies for Western Blot analysis [140]. In a study by Schmitz *et al*., only two FAS antibodies were found to detect both endogenous and exogenous FAS by Western blotting, and both were specific for intracellular epitopes of FAS [141], which were not suitable for our use, as our Fas(Y224*) does not contain the epitopes recognized by these two antibodies. To circumvent this, we first confirmed the expression of Fas in these cells by flow cytometry (FCM), with the use of both FAS and GFP antibodies (Figure 2.1 A). It is important to note that FCM did not allow us to discriminate between full length Fas and truncated Fas. We relied on the IRES sequence and the reporter protein, GFP (in the commercially available pMIG vector), to monitor the regulation of expression of both Fas genes, (Fas (Y224*) or FasWT). The IRES sequence allows for two genes to be co-expressed under the same promoter, in our case, the Fas(Y224*) (or FasWT genes) and

GFP, where the mRNA is translated into two separate proteins [140]. Recently, limitations of the IRES-linked reporter genes system have been reported and include a finding that the expression of the gene downstream of the IRES sequence is lower than the expression of the gene upstream of the IRES [142]. This should not be a problem as our Fas genes are upstream of the IRES. Another way to confirm the expression of the FasWT and the Fas(Y224*) genes would be to perform RT-PCR, with primers that recognize exogenous Fas only and also allow us to discriminate between the expression of truncated and full-length Fas. An alternative to this method would be to develop a Western antibody specific for N-terminal epitopes, which would then discriminate for the mutation we genrated. The results from our FCM analysis revealed lower expression of Fas in the FasWT E*μ-Myc* cell line in comparison to the Fas(Y224*) mutant E*μ-Myc* cell line. If the high level of Fas is indeed exogenous Fas, then the FasWT E*μ-Myc* cell line does not express high levels of additional full-length Fas, in comparison to the Fas(Y224*) cells. In spite of multiple flow cytometry-assisted cell sorts the expression of both Fas and GFP in the FasWT cells was lower than that in the Fas(Y224*) mutant cells. This could be because the overexpression of FasWT is unfavourable in the E*μ-Myc* cells, since apoptosis is triggered in cells that express high levels of *Fas*. Further evidence for this is the poor transduction efficiency of FasWT that we experienced in comparison to Fas(Y224*) (data not shown). Furthermore, when left in culture beyond 2 weeks, these cells lose their phenotype. In contrast, because we were able to overexpress Fas(Y224*) to high levels and that it had a higher transduction efficiency in E*μ-Myc* cells in comparison to the FasWT, it further confirms the role of Fas mutations in preventing apoptosis.

To optimize the *in vivo* model to circumvent all these potential problems, we are currently developing two distinct models that will both allow us to study lymphomas characteristics, regards to genotype and sensitivity to chemotherapy. One relies on the doxycycline-inducible expression of an engineered Fas insert, which we are in the early stages of optimizing, while the other will allow us to follow lymphoma development and response to therapy using a more sensitive model that relies on tracking bioluminescent lymphoma cells within live mice. The rationale for doing so is to overcome certain limitations of ultrasound measurements, such as long analysis time, inability to follow lymphoma development at early time points and overall lymph node size measurements, as opposed to tumor cell-specific measurement by

bioluminescence or fluorescence. The following chapter discusses the second model in depth.

We next investigated the effects of Fas(Y224*) and FasWT on disease progression and response to the conventional chemotherapeutic agent doxorubicin, in comparison to empty vector controls. This E*μ-Myc* mouse model of lymphoma has been very useful in elucidating drug resistance *in vivo*, and has also been used to model aggressive human lymphomas that harbor mutations in *TP53* or co-express MYC and BCL2 proteins[135,138]. For instance, this E*μ-Myc* model was previously used to show that Bcl2 expression and *Tp53* mutations could induce therapeutic resistance to lymphomas[121,135], but unlike *Fas*, the addition of Bcl2 and deletion of Tp53 did not confer a cellular growth advantage. We cannot exclude the possibility that engagement of FAS *in vivo* by its ligand, FASL, preferentially stimulated previously reported pro-survival rather that pro-apoptotic signaling, as this was not tested in this study[143]. However, given that this growth advantage occurred *in vivo* and not *in vitro* suggests that the increased growth of Fas-mutant lymphomas likely results from their ability to escape immune surveillance. Furthermore, in comparison to the control groups Fas-mutant lymphomas also had significantly delayed response (as measured by resolution of lymphadenopathy) to doxorubicin treatment. However, it is important to note that the tumor sizes in the two groups differed significantly at the treatment point. As discussed earlier, each of the injected cell types might have a different proliferation rate, resulting in an altered response in the host. Treating the Fas-mutant animals when their tumors are the same size as the other two groups could significantly modify the response to doxorubicin, which remains to be tested.

Using this model was of interest to us because it allowed for the comparison between the growth of lymphomas that differed only in their Fas genotype. The model we used also relied on the overexpression of exogenous Fas (either mutant or WT), where the relevance of such models that rely on overexpression to non-physiological levels, has been called into question[144]. However, the inclusion of the FasWT overexpression control group, and the significant growth difference observed between this group and that of the Fas(Y224*) lymphomas, allows us to make meaningful conclusions from these experiments. In future studies we plan to interrogate the role of *FAS* mutations in lymphoma progression and response to therapy, by breeding mice to generate Fas mutant lymphomas. More specifically we will breed E*μ-Myc* mice with *lpr* mice,

which feature a spontaneous genomic rearrangement in *Fas*. These mice have an early transposable element inserted in the gene, which consequently leads to premature termination and aberrant gene splicing. The resulting E*μ-Myc* mice will display one mutated Fas allele. Utilizing lymphoma cells from this genotype, we will compare their growth efficiency in immune-competent C57Bl/6 to normal E*μ-Myc* lymphoma cells. This model could confirm the importance of *Fas* status in lymphoma, allowing us to study a *Fas* mutation other than the Fas(Y224*) in a model with physiologically relevant level of *Fas* expression. This model may also shed light on the secondary genomic events that occur as a consequence of evading immune surveillance, since contrary to initial experiments using the *MYC* expressing $Arf^{-/-}$ lymphoma parental cell line (E*μ-Myc)*, here the development of lymphoma cells would occur in the context of a *Fas* mutation. Interestingly, any additional genetic alterations found in the Fas-mutant lymphomas could then be validated in our human lymphoma samples.

We confirmed that the observed aggressive growth phenotype of Fas-mutant lymphomas *in vivo* is dependent on the presence of a functional immune system, by repeating the *in vivo* Fas experiment in SCID and SCID beige mice. When injected in C57Bl/6 mice, the Fas-mutant lymphomas were larger than vector control lymphomas, however, when these same cells were injected into SCID and SCID beige mice, there was no significant difference between the tumor volumes. An interesting observation is that although not significant, the average tumor volume on day 7 was larger in the Fas-mutant group than the vector control group in the SCID mice (Figure 2.3B), however this was not the case for the SCID beige mice (Figure 2.3C). One explanation for this difference is that NK cells may, at least in part, contribute to the control of lymphoma growth through their expression of *Fasl*[145]. We solely compared lymphoma growth in these experiments, because the SCID and SCID beige mice reached humane endpoint prior to receiving treatment on Day 11. We attribute this to the lack of tumor immune surveillance in the SCID and SCID beige mice, which likely enabled the disease to progress more rapidly in these animals, in comparison to the C57Bl/6 immunocompetent controls.

This study also sheds more light on the interplay between the tumor microenvironment and the lymphoma genotype. Based on early gene expression profiling studies using unsorted biopsies, the presence of T cells in the FL microenvironment has been associated with a favorable

outcome[22]. Our results confirm findings by Afshar-Sterle *et al*., that FAS-FASL interactions are also critical in controlling lymphoma growth where T cell deficiency significantly accelerated the onset of spontaneous B cell lymphomas in mice [83]. Taken together, this work emphasizes the essential role for FAS in anti-tumor immunity. Our preliminary results demonstrate that conventional chemotherapy can engage the extrinsic apoptotic pathway through up-regulating the expression of *Fas* on malignant cells. For instance, we show that doxorubicin and cyclophosphamide treatment led to increased *Fas* expression in malignant B cells both *in vitro* and *in vivo*. This suggests that the tumor microenvironment may not only be a prognostic marker in FL, but may also actively engage malignant FL cells to potentiate chemotherapy-induced cell death. This phenomenon may explain some of the controversies over the prognostic significance of T cell subsets and macrophages in primary FL in studies that include biopsies from patients treated with different therapies. There is also strong evidence that conventional chemotherapy can elicit an anti-tumor immune response, in part by recruiting CD8+ T cells to the tumor site and increasing antigen uptake by dendritic cells, a theory known as immunogenic cell death[146,147]. More specifically, it has been shown that tumor cells can elicit an anti-tumor immune response after exposure to rituximab or anthracyclines, such as doxorubicin, both used in the treatment of FL[102,148]. It is possible that different chemotherapies stimulate the immune system in different ways and to various degrees. With this, a better understanding of the effects of chemotherapy on potentiating immune responses are necessary, and may allow us to develop better treatment regimens. Our results also challenge the widely accepted notion that conventional chemotherapy induces cell death mainly through the intrinsic apoptotic pathway and not through the extrinsic pathway, namely FAS. While early reports have noted an increase in *FAS* expression in tumor cells after exposure to chemotherapy[149-151], later experiments in mouse models showed that chemotherapy can kill primary murine lymphocytes that are deficient in functional FAS or FASL, thereby concluding that FAS is not required for chemotherapy-induced cell death[152]. This has not been however studied in the context of lymphoma, where genetic alterations such as *BCL2* overexpression and *TP53* mutations combine to inhibit the intrinsic apoptotic pathway (recall Figure 1.2). Increased FAS signaling induced by chemotherapy may potentially act to overcome the apoptotic threshold at the mitochondria, a mechanism that would be evaded by *FAS*-mutant lymphomas. In our cell lines we could not conclude that induction of *FAS* expression was due to P53 mutation status in these cell lines, as

both *TP53* mutant and WT NHL cell lines increased *FAS* expression after chemotherapy. However, this would be interesting to explore in less genetically heterogeneous models than our patient cell lines.

Patients with *FAS*-mutant lymphomas were associated with significantly inferior survival in comparison to the *FAS*WT group to HDACi. Note that the FASWT group here had rrDLBCL with a host of other mutations that contributed to the development of resistance and aggressive disease. In comparison to this heterogeneous group, *FAS*-mutant lymphomas still had significantly inferior survival. This certainly highlights the importance of further investigating *FAS* mutations in FL and rrDLBCL. In order to gain more insight into the biology of *FAS*-mutant lymphomas, we performed GEP on the primary rrDLBCL samples that revealed a potential B cell lymphoma regulatory phenotype in *FAS*-mutant lymphomas. Among the genes that were found to be more highly expressed in *FAS*-mutant lymphomas are those encoding Granzyme B and CD70. Granzyme B has been recently found to be expressed by B cells, where, in malignancies it is proposed to contribute to the suppression of the antitumor response[153-155]. Moreover CD70 overexpression has been described in many cancers[156,157] including B cell lymphomas[158] and suggested to induce cytotoxic effects in T cells and B cells and thus promote tumor escape from immune surveillance mechanisms[159]. *FAS*-mutant lymphomas were also associated with lower expression of TP53BP2 and Caspase-9. This later gene is important in the p53-dependent apoptotic pathway, where this diminution is indicative of decreased apoptosis[160]. *TP53BP2* encodes the protein ASPP2 (Apoptosis-stimulating of p53 protein 2), where low expressions levels were associated with poor clinical outcome in both DLBCL and FL[161]. Although the *FAS*-mutant signature requires further validation, it reflects our findings that *FAS* mutations are clinically relevant and associated with aggressive disease and therapeutic resistance.

Patient samples are very heterogeneous, the fact that this signature came up as significant is extremely interesting and we believe would be very important to pursue in future studies. We recognize that further validation in cell lines, either mouse models or human models using qPCR of some of these genes, such as GZMB and CD70 is also required. However, these initial experiments are promising and show that *FAS*-mutant lymphomas exhibit a B cell regulatory

phenotype, where the expression of GZMB and CD70, among other genes, may help them evade an anti-tumor immune response. To explore this phenotype, it would be very interesting to look at the number of infiltrating activated CD8+ T cells in these tumors and compare them to the FAS-WT lymphomas.

In our model, the Fas(Y224*) mutation accelerated lymphoma growth and this occurred even in the presence of the wild-type *Fas* allele. Given that *FAS* mutations were found in 15% of patients with rrDLBCL and that these patients had a significantly inferior survival, necessitates that we further study *FAS* status in future clinical studies. That *FAS*-mutant lymphomas induce a growth advantage *in vivo* but not *in vitro* and the finding that they may be associated with a B-cell regulatory phenotype, requires further research into the role of FAS in immune surveillance and also in immune-mediated response to chemotherapy. Elucidating the mechanisms that *FAS*-mutant lymphomas use to overcome anti-tumor immune responses may allow us to develop targeted, safer and more rational combinations of therapy, which harness the cytotoxicity of the neighboring immune cells and potentiate lymphoma cell death in otherwise therapy-resistant tumors.

Chapter 3: Optimization for future studies

3.1 Introduction

Chapter 3 includes results obtained from optimizing an *In Vivo* Imaging System (IVIS) model, which we expect will prove to be a better model for future studies in our lab. Both an *in vivo* fluorescence imaging model and an *in vivo* bioluminescence imaging model (BLI) of E*μ-Myc* lymphoma were developed and tested. Initial experiments revealed that BLI was by far superior to the fluorescence imaging model for the *in vivo* study of lymphoma, leading us to focus on optimizing the BLI method for future studies in our lab.

3.2 IVIS E*μ-Myc* lymphoma model

Background

The IVIS allows for non-invasive imaging of animal models of disease using either bioluminescence or fluorescence. *In vivo* BLI allows for the distribution and magnitude of luciferase expression in a live animal to be detected and evaluated, as a read-out in disease progression. Applications of *in vivo* BLI have included monitoring tumor growth and response to therapy[162,163], and studying pathogenesis in infectious disease[164]. BLI depends on knowledge of the luciferase reaction, where the substrate, D-luciferin is injected into an animal model expressing firefly luciferase, where it is oxidized by luciferase, resulting in light emission. The bioluminescence signals are then detected using a camera that visualizes luciferase activity in the animals and reports it as photons[164]. The substrate D-luciferin can be administered to animals using intraperitoneal (IP) or intravenous (IV) injection [9], and IP injection is generally preferred because of its convenience[165].

Fluorescent proteins have been recognized as reliable reporters in many applications, including *in vivo* imaging[166]. Their use in the IVIS relies on the principle of fluorescence, where put simply, light is first absorbed by the fluorescent protein which then results in the emission of longer wavelength of light, that can be detected. We chose to use *katushka* as our fluorescence reporter protein, since it is a far-red fluorescent protein that has been reported to overcome the

problem of tissue auto-fluorescence, which is primarily attributed to hemoglobin fluorescence [167]. Furthermore, *Katushka* has been shown to have no cytotoxicity[168].

Methods

We wanted to test both a fluorescence model and a bioluminescent *in vivo* imaging model, in order to first determine which was more appropriate for studying lymphoma. For the BLI we used luciferase and its substrate D-luciferin based on manufacturer's suggestions, and for the fluorescence model, we used the far-red fluorescent protein, *katushka*[168].

Luciferase and Katushka expressing cell lines

For the BLI model, we inserted the *luc2* gene[169] and replaced *GFP* with *BFP* in the same MSCV-IRES-GFP (see chapter 2) to allow for FACS. As with the Fas retroviral constructs, 293T cells were transfected with the *Luc2* construct and the pCL-ECO retrovirus packaging vector (Addgene) and two days later, their supernatants, containing Fas-expressing retrovirus, were used to infect E*μ-Myc* cells, in the presence of polybrene (4 ug/ml; Sigma). These same cells were then infected with either the *Fas*(Y224*), FasWT or the empty vector as before (see chapter 2). The infected cells were then stained with anti-FAS PE (BD) antibody, strong triple GFP-positive, BFP-positive and FAS-positive cells were sorted by FACs and allowed to grow for 48 hours on irradiated MEFs. For the vector control cells, double GFP positive and BFP positive cells were sorted by cytometry.

For the fluorescence imaging model, in each of our Fas constructs [either Fas(Y224*), FasWT or empty Vector (MSCV-IRES-GFP)], we replace *gfp* with *katushka,* creating MSCV-FAS(Y224*)-IRES-KATUSHKA, MSCV-FASWT-IRES-KATUSHKA, and MSCV-IRES-KATUSHKA, respectively. We produced virus, infected E*μ-Myc* cells the same way as described above for the luciferase-expressing cells. We sorted for *katushka* and FAS double positive cells for the two constructs. For the vector control cells, we sorted *katushka* positive cells only, which indicated the presence of our vector.

Fluorescence imaging protocol

Mice were injected with 1 million *katushka*-expressing E*μ-Myc* cells by tail vein injection. Approximately 1 hour after cell injection, mice were anesthetized with isoflurane. A control mouse (no cells) was also anesthetized and imaged. The area of the mice to be imaged (the entire ventral side) was depilated using depilatory cream (Nair; Church & Dwight). Fluorescence imaging was performed using the IVIS Spectrum system (Caliper) according to protocol provided by the manufacturer. Fluorescence images were acquired with excitation filter 570 (30 nm bandwidth) and emission filter 640 nm (20 nm bandwidth), using one second acquisition, small binning and field of view D. Multiple emission filters, excitation filters, and acquisitions lengths were also tested.

Kinetic curves and BLI protocol

To assess disease progression using this IVIS model, $1x10^6$ E*μ-Myc* luciferase-expressing-cells of each Fas genotype (mutant or vector control) were injected into the tail vein of C56Bl/6 mice (8 week old females; 5 per group, Charles River Laboratories). On day 10, the mice were injected IP with doxorubicin (10 mg/kg) or cyclophosphamide (150 mg/kg). Lymphoma growth and response to treatment were monitored with the IVIS, using biochemiluminescence as a read-out of disease progression.

The area of the mice to be imaged (the entire ventral side) was depilated using commercial depilatory cream. The luciferase substrate D-luciferin Sodium Salt (Gold biotechnology) was prepared in sterile DPBS to a final concentration of 15 mg/ml, protected from light and frozen at -80°C (for short-term storage). Bioluminescence imaging of mice was performed with the imaging settings being kept constant throughout the experiment: auto-exposure (Max exposure set to 60s), medium binning, a 2 f/stop, and field of view D. Kinetic curves were made for both the vector control (n=3) and the Fas(Y224*) mutants (n=3) lymphomas during a pilot study. D-luciferin (150 mg/kg), warmed to body temperature, was injected IP into the mice, with half the dose on each side using a 25 gauge needle and tuberculin syringes. 3 minutes post-injection, mice were placed in the induction chamber with oxygen at 0.5L flow per minute and 3.5%

isoflurane as suggested by manufacturer. Anesthetized mice were removed from the induction chamberand were positioned inside the IVIS chamber (set to 0.5L oxygen and 2% isoflurane with platform temperature of 34°C). Starting at 5 minutes post-D- luciferin injection, images were taken every 3 minutes up to 47 minutes to establish the kinetic curve as described by Burgos et al.[170].

Once the kinetic curve established, the D-luciferin injections and imaging was performed as described above for the mice experiment. Mice were imaged on day 0 (starting 1 hour post-inoculation), days 2, 4, 6, 8, 9, 10, 11, 12, 13, 14. Analysis was performed using LivingImage® 4.3.1 software. Luciferase light units were quantified in average radiance per region of interest (photons emitted/whole mouse/second).

Results and discussion

Our preliminary experiment comparing the fluorescence and bioluminescence methods of *in vivo* imaging revealed more promising results with the BLI model. Although our cells expressed *katushka*, detectable by flow cytometry and by the IVIS system, once in the mice, the software was unable to properly subtract background signal from the mice (Figure 3.1A). Reasons for this difficulty could be that the E*μ-Myc* cells were too deep in the mouse for the fluorescent signal to be properly detected, or our cells did not express high enough levels of *katushka* to be detected *in vivo*. Based on our pilot experiment and obvious challenges with the fluorescence model, we decided to focus on optimizing the BLI model. We established and honed an BLI protocol specific to our E*μ-Myc* model, wherein we determined the importance of needle size, animal positioning (and in our case flattening mice), camera settings such as field of view, as well as a stringent anesthetizing schedule in order to assure more consistent longitudinal results.

Expression of *luc2* in our E*μ-Myc* cells was successful (Figures 3.1B and 3.2B). Furthermore, the kinetic curve for both of our luciferase expressing cell lines (n=3 mice) revealed that the optimal time to image, during the plateau where the bioluminescent signal remained constant, was between 29-41 mins aftrer D-luciferin injection. We made a kinetic curve for both cell lines, as

their metabolism could differ (according to manufacturer's suggestions). Yet, the difference between the two cell lines was not significant (Figure 3.2A). As previously reported we observed that the timing of D-luciferin injection and of anesthesia after D-luciferin needed to be kept constant [171,172]. Furthermore, we determined that using 25 gauge needles and tuberculin syringes, instead of insulin syringes for D-luciferin injection reduced the occurrence of inconsistent measurements, presumed to be due to accidental intestinal injection (a known risk in intraperitoneal injection[165]. Additionally, we observed more consistent results when our mice were taped down (all limbs) during imaging, black electrical tape was selected as it did not reflect light (Figure 3.1B).

We next assessed disease progression using this BLI model of Fas(Y224*) mutant E*μ-Myc* luciferase-expressing lymphoma, in comparison to the vector control mice. We monitored disease progression in these mice and compared their response to cyclophosphamide and doxorubicin, and we calculated the percent change in biochemiluminescence and compared this between the 4 groups of mice (Figure 3.1C). In comparison to the results obtained by ultrasound in Figures 2.2 and 2.3A, the Fas(Y224*) in the BLI model did not have an aggressive phenotype in comparison to controls. Also, overall health of mice in both the Fas(Y224*) and the vector control group in the BLI model were comparable, this was not the case in the previous ultrasound experiments. One likely cause for the discrepancy is the use of two plasmids in our BLI model which we found affects overall E*μ-Myc* cell survival in culture. Another possible explanation is that expression of luciferase itself affects the E*μ-Myc* tumor development, however in a similar model, this was tested and shown to not be the case[172]. Although we thought that the BLI model will be more efficient to follow lymphoma progression, the BLI model was not suitable in the context of overexpression of Fas. We are planning on testing it on primary E*μ-Myc* cells resulting from breeding lpr mice (*Fas* mutant) with E*μ-Myc* mice*,* in order to develop *Fas*-mutant lymphomas that do not rely on Fas overexpression. In order to do so, we would transduce primary *Fas* mutant E*μ-Myc* cells, as well as control E*μ-Myc Fas*WT cells with the MSCV-LUC2-IRES-BFP vector, and then inject them into recipient mice. This future experiment could overcome potential problems with expressing two plasmids in our current BLI model, and also would allow us to explore the effect of *Fas* mutations on lymphoma growth in a non-overexpression model.

A **B**

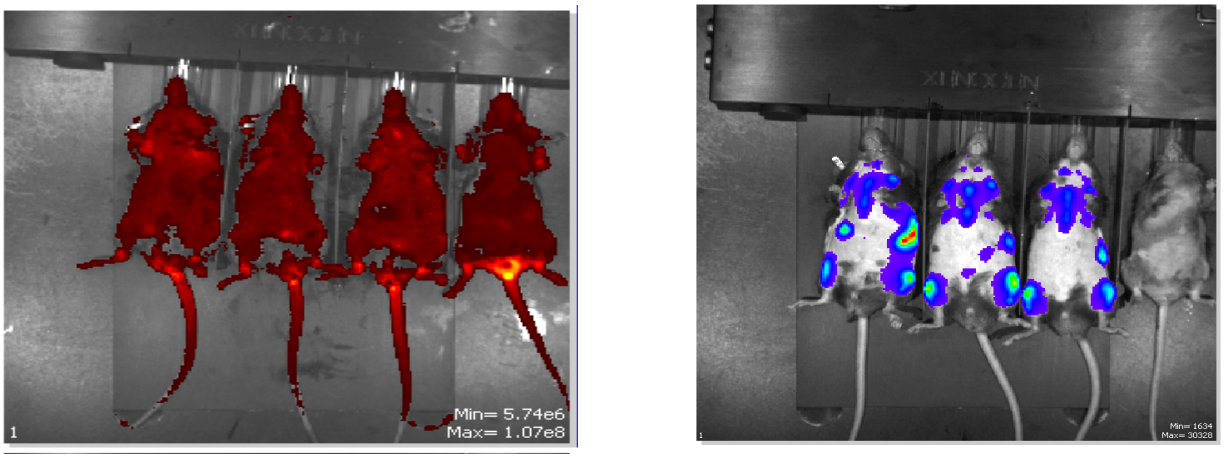

Figure 3.1. Pilot experiment reveals BLI is more appropriate for E*μ*-*Myc* lymphoma
Superimposed photographs of mice and fluorescent signal (A) or bioluminescent signal (B). The mouse on the far right is a control mouse without cell injection in both images. Background subtraction of animal autofluorescence has been performed. Images shown were day 0, 1 hour after cell injection, but are reflective of all other imaging days (4, 7 and 12).

A

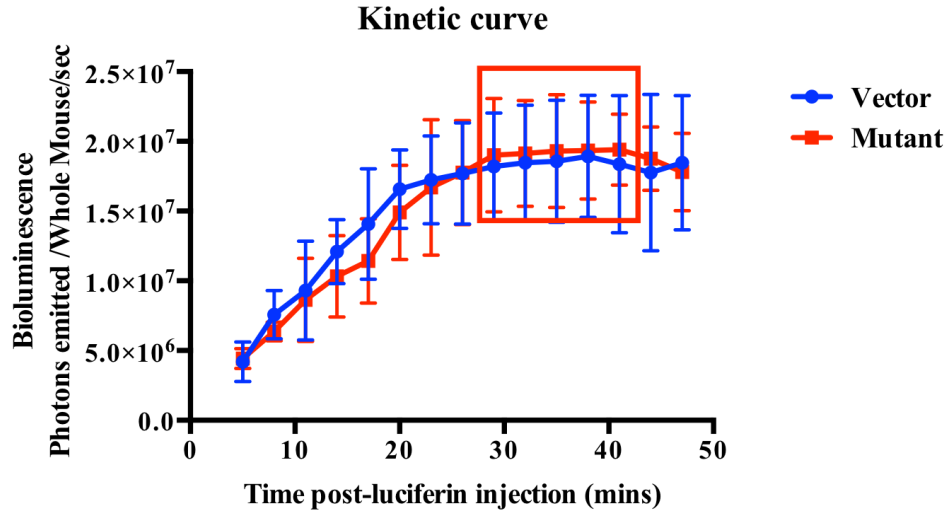
Kinetic curve
Bioluminescence
Photons emitted /Whole Mouse/sec
2.5×10^7
2.0×10^7
1.5×10^7
1.0×10^7
5.0×10^6
0.0
0
10
20
30
40
50
Time post-luciferin injection (mins)
Vector
Mutant

B

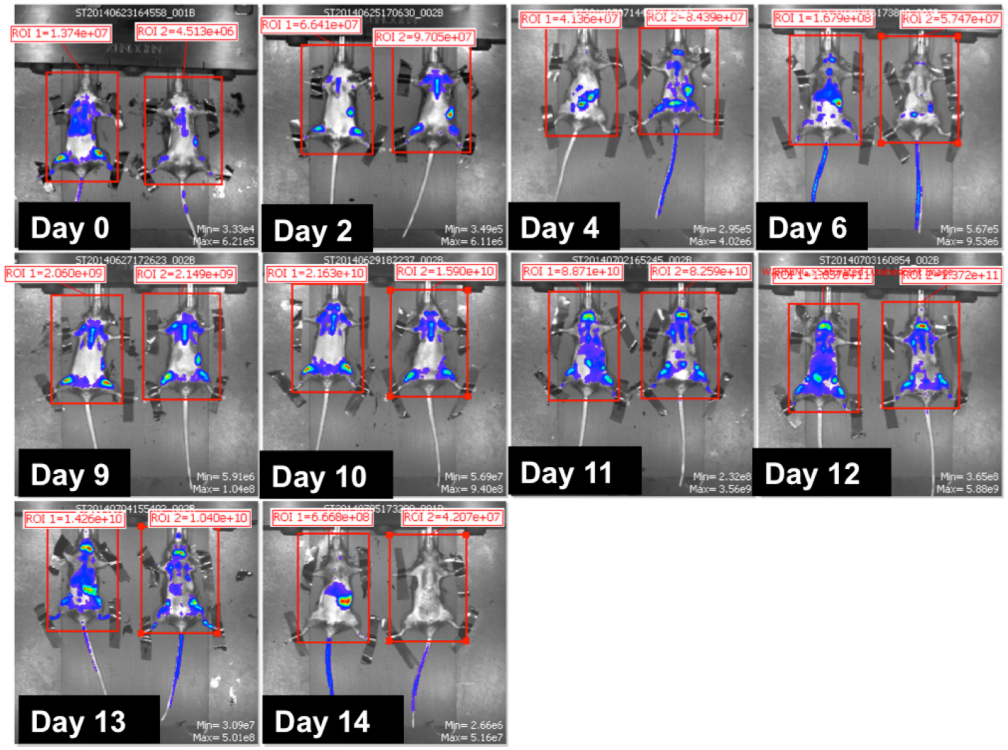
Day 0
Day 2
Day 4
Day 6
Day 9
Day 10
Day 11
Day 12
Day 13
Day 14

C

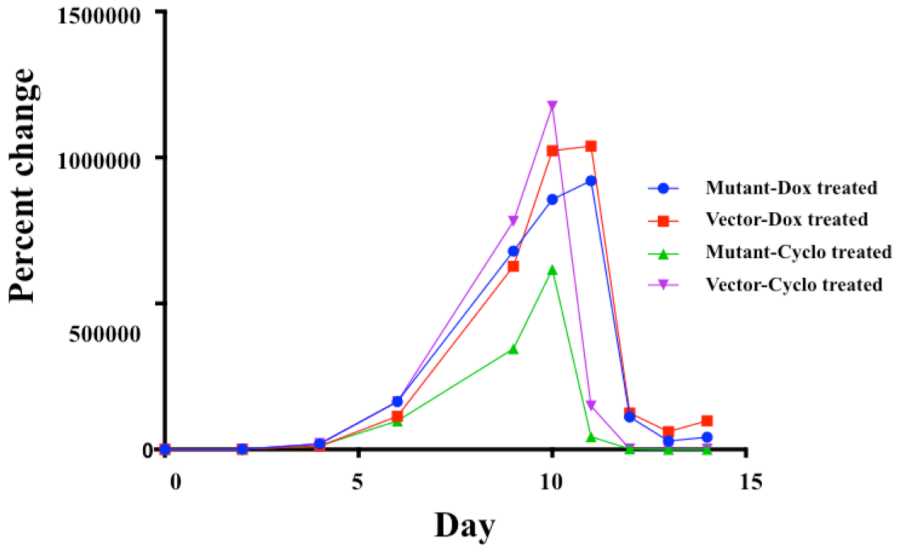
Percent change
1500000
1000000
500000
0
0
5
10
15
Day
Mutant-Dox treated
Vector-Dox treated
Mutant-Cyclo treated
Vector-Cyclo treated

Figure 3.2. Optimization of BLI E*μ-Myc* lymphoma model.
A) Kinetic curve of photons emitted per mouse imaged every three minutes starting at 5 minutes post intraperitoneal injection of D-luciferin. Kinetic curve was made for both luciferase expressing cell types, namely, E*μ-Myc* vector control and Fas(Y224*) cells. Red box indicates the signal plateau, where imaging mice is best, for reproducible results throughout the longitudinal study. B) Representative image of mice in the longitudinal study. Note every image is on a separate scale. Both mice shown have been injected with vector control cells. C) Results from longitudinal study where tumor growth is expressed as percent change of photons emitted in both Fas(Y224*) mutant and vector control groups that were treated with either cyclophosphamide or doxorubicin.

Chapter 4: Conclusion and Summary

It has become increasingly evident in the literature that some chemotherapeutic agents can elicit an anti-tumor immune response in addition to their cytotoxic effects[83,96,97,173]. Furthermore, it has been recently shown that CD8+ T cell can prevent spontaneous B cell lymphoma development in a FAS-FASL-dependent manner[83]. Although *FAS* mutations have been reported in TLy including the *FAS*(Y232*) mutation[30], they have not been studied in the context of therapeutic resistance. Furthermore, to our knowledge we are the first to demonstrate that a single mutation in *FAS* is sufficient to accelerate lymphoma progression prior to chemotherapy.

In Chapter 2 we aimed to characterize the role of *FAS* mutations using an *in vivo* murine lymphoma model. First, we transduced the E*μ-Myc* cell line with either Fas(Y224*), FasWT or vector control. *In vitro* studies on these three cell lines revealed no innate differences in growth characteristics or sensitivity to chemotherapy, mimicking our earlier findings with human cell lines. However, when three groups of immunocompetent C57Bl/6 mice were injected with these E*μ-Myc* lymphoma cells (differing only in their Fas genotype), Fas(Y224*) was found to dramatically increase tumor growth in comparison to controls. By injecting these cells into SCID and SCID beige mice, we showed the aggressive phenotype of Fas(Y224*) required a functional immune system. This is not surprising considering the reliance on FAS-FASL interactions for FAS signaling.

In the cohort of patients with rrDLBCL, 15 % (5/33) were found to have *FAS* mutations, which were associated with an inferior survival after treatment with the HDACi panobinostat ($p>0.001$). Gene set enrichment analysis (GSEA) using gene expression data from the BJAB cell lines and patient lymphomas, comparing altered gene expression in *FAS*-mutant and *FAS*-WT lymphomas, led to the identification of a potential *FAS*-mutant lymphoma signature, where *FAS*-mutant lymphoma cells may take on a regulatory B cell phenotype. The expression Granzyme B and FASL, and other such genes may suppress surrounding anti-tumor immune cells, possibly contributing to the aggressive phenotype of *FAS*-mutant lymphomas.

Supporting the concept of an immune response induced after chemotherapy, we observed *FAS* to be up-regulated in malignant B cells after treatment with cyclophosphamide and doxorubicin *in*

vivo and etoposide and doxorubicin in human cell lines in vitro. This is accordance with early studies that found an increase in *FAS* expression in tumor cells after exposure to chemotherapy [149-151]. However, later experiments in mouse models showed that chemotherapy can kill primary murine lymphocytes that are deficient in functional FAS or FASL, thereby concluding that FAS is not required for chemotherapy-induced cell death[152]. The effect *FAS* mutations may therefore be context-dependent, and we hypothesize that *FAS* mutations may be clinically important in FL since the intrinsic pathway is blocked by over-expression of BCL2 or p53 mutations.

In Chapter 3 we aimed to optimize an IVIS model to better study chemotherapeutic resistance in NHL. In comparing both fluorescence and bioluminescent models, we determined that bioluminescence was more appropriate for the study of lymphoma. We expect that the IVIS method will allow us to gain further insight into chemotherapeutic resistant lymphomas, including *FAS*-mutant lymphomas. In this additional chapter we also explored some of the challenges we faced in studying *FAS*-mutant lymphomas with this model and rationale for future work.

We showed that mutations in *FAS* can be clinically important in patients with FL by promoting lymphoma growth and inducing therapeutic resistance. The full malignant phenotype of *FAS*-mutant lymphomas could only be elicited *in vivo,* and not *in vitro,* suggesting that a FAS-mediated immune response controls lymphoma growth and actively participates in chemotherapy-induced lymphoma cell death. Furthermore, our study highlights the importance of using appropriate model systems. Better understanding the interactions between *FAS* mutations and the microenvironment could lead to identification of novel therapeutic targets.

Although progress has been made in the treatment of follicular lymphoma in recent years, chemotherapeutic resistance remains a significant problem. With this, the identification of mutations associated with therapeutic resistance and disease progression could serve to help guide clinicians in the treatment of these patients. Furthermore, elucidating the mechanisms of resistance, may allow for the development and/or identification of therapies that could be effective against these otherwise resistant lymphomas.

References

1. Statistics CCSsSCoC. Canadian Cancer Statistics 2011. Toronto: Canadian Cancer Society; 2011. 16 p.
2. Anderson JR, Armitage JO, Weisenburger DD. Epidemiology of the non-Hodgkin's lymphomas: distributions of the major subtypes differ by geographic locations. Non-Hodgkin's Lymphoma Classification Project. Ann Oncol 1998;9(7):717-20.
3. Kridel R, Sehn LH, Gascoyne RD. Pathogenesis of follicular lymphoma. J Clin Invest 2012;122(10):3424-31.
4. Victora GD, Nussenzweig MC. Germinal centers. Annu Rev Immunol 2012;30:429-57.
5. Horning SJ, Rosenberg SA. The natural history of initially untreated low-grade non-Hodgkin's lymphomas. N Engl J Med 1984;311(23):1471-5.
6. van Besien K, Schouten H. Follicular lymphoma: a historical overview. Leuk Lymphoma 2007;48(2):232-43.
7. Sabattini E, Bacci F, Sagramoso C, Pileri SA. WHO classification of tumours of haematopoietic and lymphoid tissues in 2008: an overview. Pathologica 2010;102(3):83-7.
8. Kritharis A, Sharma J, Evens AM. Current therapeutic strategies and new treatment paradigms for follicular lymphoma. Cancer Treat Res 2015;165:197-226.
9. Lossos IS, Gascoyne RD. Transformation of follicular lymphoma. Best Pract Res Clin Haematol 2011;24(2):147-63.
10. Cheung MC, Imrie KR. Targeting the follicular lymphoma microenvironment - ready for prime-time? Leuk Lymphoma 2008;49(5):837-8.
11. Casulo C, Burack WR, Friedberg JW. Transformed follicular non-Hodgkin lymphoma. Blood 2015;125(1):40-7.
12. Diaz-Alderete A, Doval A, Camacho F, Verde L, Sabin P, Arranz-Saez R, Bellas C, Corbacho C, Gil J, Perez-Martin M and others. Frequency of BCL2 and BCL6 translocations in follicular lymphoma: relation with histological and clinical features. Leuk Lymphoma 2008;49(1):95-101.
13. Ji W, Qu GZ, Ye P, Zhang XY, Halabi S, Ehrlich M. Frequent detection of bcl-2/JH translocations in human blood and organ samples by a quantitative polymerase chain reaction assay. Cancer Res 1995;55(13):2876-82.
14. Friedberg JW. Double hit diffuse large B-cell lymphomas: diagnostic and therapeutic challenges. Chin Clin Oncol 2015;4(1):9.
15. Hardianti MS, Tatsumi E, Syampurnawati M, Furuta K, Saigo K, Nakamachi Y, Kumagai S, Ohno H, Tanabe S, Uchida M and others. Activation-induced cytidine deaminase expression in follicular lymphoma: association between AID expression and ongoing mutation in FL. Leukemia 2004;18(4):826-31.
16. Roulland S, Faroudi M, Mamessier E, Sungalee S, Salles G, Nadel B. Early steps of follicular lymphoma pathogenesis. Adv Immunol 2011;111:1-46.
17. Keim C, Kazadi D, Rothschild G, Basu U. Regulation of AID, the B-cell genome mutator. Genes Dev 2013;27(1):1-17.
18. Yunis JJ, Frizzera G, Oken MM, McKenna J, Theologides A, Arnesen M. Multiple recurrent genomic defects in follicular lymphoma. A possible model for cancer. N Engl J Med 1987;316(2):79-84.

19. Relander T, Johnson NA, Farinha P, Connors JM, Sehn LH, Gascoyne RD. Prognostic factors in follicular lymphoma. J Clin Oncol 2010;28(17):2902-13.
20. Morin RD, Johnson NA, Severson TM, Mungall AJ, An J, Goya R, Paul JE, Boyle M, Woolcock BW, Kuchenbauer F and others. Somatic mutation of EZH2 (Y641) in Follicular and Diffuse Large B-cell Lymphomas of Germinal Center Origin. Nat Genet 2010;42(2):181-5.
21. Green MR, Kihira S, Liu CL, Nair RV, Salari R, Gentles AJ, Irish J, Stehr H, Vicente-Duenas C, Romero-Camarero I and others. Mutations in early follicular lymphoma progenitors are associated with suppressed antigen presentation. Proc Natl Acad Sci U S A 2015;112(10):E1116-25.
22. Dave SS, Wright G, Tan B, Rosenwald A, Gascoyne RD, Chan WC, Fisher RI, Braziel RM, Rimsza LM, Grogan TM and others. Prediction of survival in follicular lymphoma based on molecular features of tumor-infiltrating immune cells. N Engl J Med 2004;351(21):2159-69.
23. Scott DW, Gascoyne RD. The tumour microenvironment in B cell lymphomas. Nat Rev Cancer 2014;14(8):517-34.
24. Ferry JA. Burkitt's lymphoma: clinicopathologic features and differential diagnosis. Oncologist 2006;11(4):375-83.
25. Montoto S, Davies AJ, Matthews J, Calaminici M, Norton AJ, Amess J, Vinnicombe S, Waters R, Rohatiner AZ, Lister TA. Risk and clinical implications of transformation of follicular lymphoma to diffuse large B-cell lymphoma. J Clin Oncol 2007;25(17):2426-33.
26. Villuendas R, Sanchez-Beato M, Martinez JC, Saez AI, Martinez-Delgado B, Garcia JF, Mateo MS, Sanchez-Verde L, Benitez J, Martinez P and others. Loss of p16/INK4A protein expression in non-Hodgkin's lymphomas is a frequent finding associated with tumor progression. Am J Pathol 1998;153(3):887-97.
27. Zilfou JT, Lowe SW. Tumor Suppressive Functions of p53. Cold Spring Harb Perspect Biol 2009;1(5).
28. Robles AI, Harris CC. Clinical Outcomes and Correlates of TP53 Mutations and Cancer. Cold Spring Harb Perspect Biol 2010;2(3).
29. Leroy K, Haioun C, Lepage E, Le Metayer N, Berger F, Labouyrie E, Meignin V, Petit B, Bastard C, Salles G and others. p53 gene mutations are associated with poor survival in low and low-intermediate risk diffuse large B-cell lymphomas. Ann Oncol 2002;13(7):1108-15.
30. Pasqualucci L, Khiabanian H, Fangazio M, Vasishtha M, Messina M, Holmes AB, Ouillette P, Trifonov V, Rossi D, Tabbo F and others. Genetics of follicular lymphoma transformation. Cell Rep 2014;6(1):130-40.
31. Rosenwald A, Wright G, Chan WC, Connors JM, Campo E, Fisher RI, Gascoyne RD, Muller-Hermelink HK, Smeland EB, Giltnane JM and others. The use of molecular profiling to predict survival after chemotherapy for diffuse large-B-cell lymphoma. N Engl J Med 2002;346(25):1937-47.
32. Salles G, Seymour JF, Offner F, Lopez-Guillermo A, Belada D, Xerri L, Feugier P, Bouabdallah R, Catalano JV, Brice P and others. Rituximab maintenance for 2 years in patients with high tumour burden follicular lymphoma responding to rituximab plus chemotherapy (PRIMA): a phase 3, randomised controlled trial. Lancet 2011;377(9759):42-51.

33. Sehn LH, Gascoyne RD. Diffuse large B-cell lymphoma: optimizing outcome in the context of clinical and biologic heterogeneity. Blood 2015;125(1):22-32.
34. Sidman CL, Shaffer DJ, Jacobsen K, Vargas SR, Osmond DG. Cell populations during tumorigenesis in Eu-myc transgenic mice. Leukemia 1993;7(6):887-95.
35. Rempel RE, Jiang X, Fullerton P, Tan TZ, Ye J, Lau JA, Mori S, Chi JT, Nevins JR, Friedman DR. Utilization of the Emu-Myc mouse to model heterogeneity of therapeutic response. Mol Cancer Ther 2014;13(12):3219-29.
36. Adams JM, Harris AW, Pinkert CA, Corcoran LM, Alexander WS, Cory S, Palmiter RD, Brinster RL. The c-myc oncogene driven by immunoglobulin enhancers induces lymphoid malignancy in transgenic mice. Nature 1985;318(6046):533-8.
37. Burgess DJ, Doles J, Zender L, Xue W, Ma B, McCombie WR, Hannon GJ, Lowe SW, Hemann MT. Topoisomerase levels determine chemotherapy response in vitro and in vivo. Proc Natl Acad Sci U S A 2008;105(26):9053-8.
38. Dokmanovic M, Clarke C, Marks PA. Histone deacetylase inhibitors: overview and perspectives. Mol Cancer Res 2007;5(10):981-9.
39. Rangwala S, Zhang C, Duvic M. HDAC inhibitors for the treatment of cutaneous T-cell lymphomas. Future Med Chem 2012;4(4):471-86.
40. Ouyang L, Shi Z, Zhao S, Wang FT, Zhou TT, Liu B, Bao JK. Programmed cell death pathways in cancer: a review of apoptosis, autophagy and programmed necrosis. Cell Prolif 2012;45(6):487-98.
41. Kerr JF, Wyllie AH, Currie AR. Apoptosis: a basic biological phenomenon with wide-ranging implications in tissue kinetics. Br J Cancer 1972;26(4):239-57.
42. Zaman S, Wang R, Gandhi V. Targeting the apoptosis pathway in hematologic malignancies. Leuk Lymphoma 2014;55(9):1980-92.
43. Trapani JA, Smyth MJ. Functional significance of the perforin/granzyme cell death pathway. Nat Rev Immunol 2002;2(10):735-47.
44. Nicholson DW, Thornberry NA. Caspases: killer proteases. Trends Biochem Sci 1997;22(8):299-306.
45. Martinvalet D, Zhu P, Lieberman J. Granzyme A induces caspase-independent mitochondrial damage, a required first step for apoptosis. Immunity 2005;22(3):355-70.
46. Boatright KM, Salvesen GS. Mechanisms of caspase activation. Curr Opin Cell Biol 2003;15(6):725-31.
47. Cohen GM. Caspases: the executioners of apoptosis. Biochem J 1997;326 (Pt 1):1-16.
48. Slee EA, Adrain C, Martin SJ. Executioner caspase-3, -6, and -7 perform distinct, non-redundant roles during the demolition phase of apoptosis. J Biol Chem 2001;276(10):7320-6.
49. Nowsheen S, Yang ES. The intersection between DNA damage response and cell death pathways. Exp Oncol 2012;34(3):243-54.
50. Cory S, Adams JM. The Bcl2 family: regulators of the cellular life-or-death switch. Nat Rev Cancer 2002;2(9):647-56.
51. Lomonosova E, Chinnadurai G. BH3-only proteins in apoptosis and beyond: an overview. Oncogene 2008;27 Suppl 1:S2-19.
52. Sarosiek KA, Chi X, Bachman JA, Sims JJ, Montero J, Patel L, Flanagan A, Andrews DW, Sorger P, Letai A. BID preferentially activates BAK while BIM preferentially activates BAX, affecting chemotherapy response. Mol Cell 2013;51(6):751-65.
53. Yip KW, Reed JC. Bcl-2 family proteins and cancer. Oncogene 2008;27(50):6398-406.

54. Locksley RM, Killeen N, Lenardo MJ. The TNF and TNF receptor superfamilies: integrating mammalian biology. Cell 2001;104(4):487-501.
55. Walczak H, Krammer PH. The CD95 (APO-1/Fas) and the TRAIL (APO-2L) apoptosis systems. Exp Cell Res 2000;256(1):58-66.
56. Muzio M, Chinnaiyan AM, Kischkel FC, O'Rourke K, Shevchenko A, Ni J, Scaffidi C, Bretz JD, Zhang M, Gentz R and others. FLICE, a novel FADD-homologous ICE/CED-3-like protease, is recruited to the CD95 (Fas/APO-1) death--inducing signaling complex. Cell 1996;85(6):817-27.
57. Hsu H, Shu HB, Pan MG, Goeddel DV. TRADD-TRAF2 and TRADD-FADD interactions define two distinct TNF receptor 1 signal transduction pathways. Cell 1996;84(2):299-308.
58. Lavrik IN, Krammer PH. Regulation of CD95/Fas signaling at the DISC. Cell Death Differ 2012;19(1):36-41.
59. Yonehara S, Ishii A, Yonehara M. A cell-killing monoclonal antibody (anti-Fas) to a cell surface antigen co-downregulated with the receptor of tumor necrosis factor. J Exp Med 1989;169(5):1747-56.
60. Trauth BC, Klas C, Peters AM, Matzku S, Moller P, Falk W, Debatin KM, Krammer PH. Monoclonal antibody-mediated tumor regression by induction of apoptosis. Science 1989;245(4915):301-5.
61. Itoh N, Yonehara S, Ishii A, Yonehara M, Mizushima S, Sameshima M, Hase A, Seto Y, Nagata S. The polypeptide encoded by the cDNA for human cell surface antigen Fas can mediate apoptosis. Cell 1991;66(2):233-43.
62. Orlinick JR, Vaishnaw A, Elkon KB, Chao MV. Requirement of cysteine-rich repeats of the Fas receptor for binding by the Fas ligand. J Biol Chem 1997;272(46):28889-94.
63. Sessler T, Healy S, Samali A, Szegezdi E. Structural determinants of DISC function: new insights into death receptor-mediated apoptosis signalling. Pharmacol Ther 2013;140(2):186-99.
64. Watanabe-Fukunaga R, Brannan CI, Itoh N, Yonehara S, Copeland NG, Jenkins NA, Nagata S. The cDNA structure, expression, and chromosomal assignment of the mouse Fas antigen. J Immunol 1992;148(4):1274-9.
65. Watanabe D, Suda T, Nagata S. Expression of Fas in B cells of the mouse germinal center and Fas-dependent killing of activated B cells. Int Immunol 1995;7(12):1949-56.
66. Suda T, Okazaki T, Naito Y, Yokota T, Arai N, Ozaki S, Nakao K, Nagata S. Expression of the Fas ligand in cells of T cell lineage. J Immunol 1995;154(8):3806-13.
67. Chua HL, Serov Y, Brahmi Z. Regulation of FasL expression in natural killer cells. Hum Immunol 2004;65(4):317-27.
68. Hao Z, Duncan GS, Seagal J, Su YW, Hong C, Haight J, Chen NJ, Elia A, Wakeham A, Li WY and others. Fas receptor expression in germinal-center B cells is essential for T and B lymphocyte homeostasis. Immunity 2008;29(4):615-27.
69. Fouque A, Debure L, Legembre P. The CD95/CD95L signaling pathway: a role in carcinogenesis. Biochim Biophys Acta 2014;1846(1):130-41.
70. Hanabuchi S, Koyanagi M, Kawasaki A, Shinohara N, Matsuzawa A, Nishimura Y, Kobayashi Y, Yonehara S, Yagita H, Okumura K. Fas and its ligand in a general mechanism of T-cell-mediated cytotoxicity. Proceedings of the National Academy of Sciences of the United States of America 1994;91(11):4930-4.
71. Nagata S, Golstein P. The Fas death factor. Science 1995;267(5203):1449-56.

72. Wang L, Yang JK, Kabaleeswaran V, Rice AJ, Cruz AC, Park AY, Yin Q, Damko E, Jang SB, Raunser S and others. The Fas-FADD death domain complex structure reveals the basis of DISC assembly and disease mutations. Nat Struct Mol Biol 2010;17(11):1324-9.
73. Nagata S. Apoptosis by death factor. Cell 1997;88(3):355-65.
74. Peter ME, Budd RC, Desbarats J, Hedrick SM, Hueber AO, Newell MK, Owen LB, Pope RM, Tschopp J, Wajant H and others. The CD95 receptor: apoptosis revisited. Cell 2007;129(3):447-50.
75. Grassme H, Jekle A, Riehle A, Schwarz H, Berger J, Sandhoff K, Kolesnick R, Gulbins E. CD95 signaling via ceramide-rich membrane rafts. J Biol Chem 2001;276(23):20589-96.
76. Gajate C, Mollinedo F. Lipid rafts and raft-mediated supramolecular entities in the regulation of CD95 death receptor apoptotic signaling. Apoptosis 2015;20(5):584-606.
77. Muppidi JR, Siegel RM. Ligand-independent redistribution of Fas (CD95) into lipid rafts mediates clonotypic T cell death. Nat Immunol 2004;5(2):182-9.
78. Mollinedo F, Gajate C. Lipid rafts as major platforms for signaling regulation in cancer. Adv Biol Regul 2015;57:130-46.
79. Stel AJ, Ten Cate B, Jacobs S, Kok JW, Spierings DC, Dondorff M, Helfrich W, Kluin-Nelemans HC, de Leij LF, Withoff S and others. Fas receptor clustering and involvement of the death receptor pathway in rituximab-mediated apoptosis with concomitant sensitization of lymphoma B cells to fas-induced apoptosis. J Immunol 2007;178(4):2287-95.
80. Hanahan D, Weinberg RA. Hallmarks of cancer: the next generation. Cell 2011;144(5):646-74.
81. Shimizu M, Fontana A, Takeda Y, Yoshimoto T, Tsubura A, Matsuzawa A. Fas/Apo-1 (CD95)-mediated apoptosis of neutrophils with Fas ligand (CD95L)-expressing tumors is crucial for induction of inflammation by neutrophilic polymorphonuclear leukocytes associated with antitumor immunity. Cell Immunol 2001;207(1):41-8.
82. Kim R, Emi M, Tanabe K. Cancer immunoediting from immune surveillance to immune escape. Immunology 2007;121(1):1-14.
83. Afshar-Sterle S, Zotos D, Bernard NJ, Scherger AK, Rodling L, Alsop AE, Walker J, Masson F, Belz GT, Corcoran LM and others. Fas ligand-mediated immune surveillance by T cells is essential for the control of spontaneous B cell lymphomas. Nat Med 2014;20(3):283-90.
84. O'Connell J, O'Sullivan GC, Collins JK, Shanahan F. The Fas counterattack: Fas-mediated T cell killing by colon cancer cells expressing Fas ligand. J Exp Med 1996;184(3):1075-82.
85. Motz GT, Santoro SP, Wang LP, Garrabrant T, Lastra RR, Hagemann IS, Lal P, Feldman MD, Benencia F, Coukos G. Tumor endothelium FasL establishes a selective immune barrier promoting tolerance in tumors. Nat Med 2014;20(6):607-15.
86. Ivanov VN, Bhoumik A, Krasilnikov M, Raz R, Owen-Schaub LB, Levy D, Horvath CM, Ronai Z. Cooperation between STAT3 and c-jun suppresses Fas transcription. Mol Cell 2001;7(3):517-28.
87. Huang SK, Scruggs AM, Donaghy J, Horowitz JC, Zaslona Z, Przybranowski S, White ES, Peters-Golden M. Histone modifications are responsible for decreased Fas expression and apoptosis resistance in fibrotic lung fibroblasts. Cell Death Dis 2013;4:e621.

88. Cheng J, Zhou T, Liu C, Shapiro JP, Brauer MJ, Kiefer MC, Barr PJ, Mountz JD. Protection from Fas-mediated apoptosis by a soluble form of the Fas molecule. Science 1994;263(5154):1759-62.
89. Kojima Y, Tsurumi H, Goto N, Shimizu M, Kasahara S, Yamada T, Kanemura N, Hara T, Sawada M, Saio M and others. Fas and Fas ligand expression on germinal center type-diffuse large B-cell lymphoma is associated with the clinical outcome. Eur J Haematol 2006;76(6):465-72.
90. Igney FH, Krammer PH. Death and anti-death: tumour resistance to apoptosis. Nat Rev Cancer 2002;2(4):277-88.
91. Richardson DS, Allen PD, Kelsey SM, Newland AC. Inhibition of FAS/FAS-ligand does not block chemotherapy-induced apoptosis in drug sensitive and resistant cells. Adv Exp Med Biol 1999;457:259-66.
92. Eischen CM, Kottke TJ, Martins LM, Basi GS, Tung JS, Earnshaw WC, Leibson PJ, Kaufmann SH. Comparison of apoptosis in wild-type and Fas-resistant cells: chemotherapy-induced apoptosis is not dependent on Fas/Fas ligand interactions. Blood 1997;90(3):935-43.
93. Happo L, Cragg MS, Phipson B, Haga JM, Jansen ES, Herold MJ, Dewson G, Michalak EM, Vandenberg CJ, Smyth GK and others. Maximal killing of lymphoma cells by DNA damage-inducing therapy requires not only the p53 targets Puma and Noxa, but also Bim. Blood 2010;116(24):5256-67.
94. Friesen C, Herr I, Krammer PH, Debatin KM. Involvement of the CD95 (APO-1/FAS) receptor/ligand system in drug-induced apoptosis in leukemia cells. Nat Med 1996;2(5):574-7.
95. Friesen C, Fulda S, Debatin KM. Deficient activation of the CD95 (APO-1/Fas) system in drug-resistant cells. Leukemia 1997;11(11):1833-41.
96. Kroemer G, Galluzzi L, Kepp O, Zitvogel L. Immunogenic cell death in cancer therapy. Annu Rev Immunol 2013;31:51-72.
97. Obeid M, Panaretakis T, Tesniere A, Joza N, Tufi R, Apetoh L, Ghiringhelli F, Zitvogel L, Kroemer G. Leveraging the immune system during chemotherapy: moving calreticulin to the cell surface converts apoptotic death from "silent" to immunogenic. Cancer Res 2007;67(17):7941-4.
98. Galluzzi L, Senovilla L, Zitvogel L, Kroemer G. The secret ally: immunostimulation by anticancer drugs. Nat Rev Drug Discov 2012;11(3):215-33.
99. Michaud M, Martins I, Sukkurwala AQ, Adjemian S, Ma Y, Pellegatti P, Shen S, Kepp O, Scoazec M, Mignot G and others. Autophagy-dependent anticancer immune responses induced by chemotherapeutic agents in mice. Science 2011;334(6062):1573-7.
100. Ghiringhelli F, Apetoh L, Tesniere A, Aymeric L, Ma Y, Ortiz C, Vermaelen K, Panaretakis T, Mignot G, Ullrich E and others. Activation of the NLRP3 inflammasome in dendritic cells induces IL-1beta-dependent adaptive immunity against tumors. Nat Med 2009;15(10):1170-8.
101. Apetoh L, Ghiringhelli F, Tesniere A, Obeid M, Ortiz C, Criollo A, Mignot G, Maiuri MC, Ullrich E, Saulnier P and others. Toll-like receptor 4-dependent contribution of the immune system to anticancer chemotherapy and radiotherapy. Nat Med 2007;13(9):1050-9.
102. Casares N, Pequignot MO, Tesniere A, Ghiringhelli F, Roux S, Chaput N, Schmitt E, Hamai A, Hervas-Stubbs S, Obeid M and others. Caspase-dependent immunogenicity of

doxorubicin-induced tumor cell death. The Journal of experimental medicine 2005;202(12):1691-701.
103. Bracci L, Schiavoni G, Sistigu A, Belardelli F. Immune-based mechanisms of cytotoxic chemotherapy: implications for the design of novel and rationale-based combined treatments against cancer. Cell Death Differ 2014;21(1):15-25.
104. Poppema S, Maggio E, van den Berg A. Development of lymphoma in Autoimmune Lymphoproliferative Syndrome (ALPS) and its relationship to Fas gene mutations. Leuk Lymphoma 2004;45(3):423-31.
105. Straus SE, Sneller M, Lenardo MJ, Puck JM, Strober W. An inherited disorder of lymphocyte apoptosis: the autoimmune lymphoproliferative syndrome. Ann Intern Med 1999;130(7):591-601.
106. Yokota A, Takeuchi E, Iizuka M, Ikegami Y, Takayama H, Shinohara N. Prominent dominant negative effect of a mutant Fas molecule lacking death domain on cell-mediated induction of apoptosis. Mol Immunol 2005;42(1):71-8.
107. Takahashi T, Tanaka M, Brannan CI, Jenkins NA, Copeland NG, Suda T, Nagata S. Generalized lymphoproliferative disease in mice, caused by a point mutation in the Fas ligand. Cell 1994;76(6):969-76.
108. Cohen PL, Eisenberg RA. Lpr and gld: single gene models of systemic autoimmunity and lymphoproliferative disease. Annu Rev Immunol 1991;9:243-69.
109. Watanabe-Fukunaga R, Brannan CI, Copeland NG, Jenkins NA, Nagata S. Lymphoproliferation disorder in mice explained by defects in Fas antigen that mediates apoptosis. Nature 1992;356(6367):314-7.
110. Landowski TH, Qu N, Buyuksal I, Painter JS, Dalton WS. Mutations in the Fas antigen in patients with multiple myeloma. Blood 1997;90(11):4266-70.
111. Tamiya S, Etoh K, Suzushima H, Takatsuki K, Matsuoka M. Mutation of CD95 (Fas/Apo-1) gene in adult T-cell leukemia cells. Blood 1998;91(10):3935-42.
112. Beltinger C, Kurz E, Bohler T, Schrappe M, Ludwig WD, Debatin KM. CD95 (APO-1/Fas) mutations in childhood T-lineage acute lymphoblastic leukemia. Blood 1998;91(10):3943-51.
113. Gronbaek K, Straten PT, Ralfkiaer E, Ahrenkiel V, Andersen MK, Hansen NE, Zeuthen J, Hou-Jensen K, Guldberg P. Somatic Fas mutations in non-Hodgkin's lymphoma: association with extranodal disease and autoimmunity. Blood 1998;92(9):3018-24.
114. Lee SH, Shin MS, Park WS, Kim SY, Dong SM, Pi JH, Lee HK, Kim HS, Jang JJ, Kim CS and others. Alterations of Fas (APO-1/CD95) gene in transitional cell carcinomas of urinary bladder. Cancer Res 1999;59(13):3068-72.
115. Park WS, Oh RR, Kim YS, Park JY, Lee SH, Shin MS, Kim SY, Kim PJ, Lee HK, Yoo NY and others. Somatic mutations in the death domain of the Fas (Apo-1/CD95) gene in gastric cancer. J Pathol 2001;193(2):162-8.
116. Shin MS, Park WS, Kim SY, Kim HS, Kang SJ, Song KY, Park JY, Dong SM, Pi JH, Oh RR and others. Alterations of Fas (Apo-1/CD95) gene in cutaneous malignant melanoma. Am J Pathol 1999;154(6):1785-91.
117. Lee SH, Shin MS, Park WS, Kim SY, Kim HS, Han JY, Park GS, Dong SM, Pi JH, Kim CS and others. Alterations of Fas (Apo-1/CD95) gene in non-small cell lung cancer. Oncogene 1999;18(25):3754-60.

118. Pasqualucci L, Trifonov V, Fabbri G, Ma J, Rossi D, Chiarenza A, Wells VA, Grunn A, Messina M, Elliot O and others. Analysis of the coding genome of diffuse large B-cell lymphoma. Nat Genet 2011;43(9):830-7.
119. Morin RD, Mendez-Lago M, Mungall AJ, Goya R, Mungall KL, Corbett RD, Johnson NA, Severson TM, Chiu R, Field M and others. Frequent mutation of histone-modifying genes in non-Hodgkin lymphoma. Nature 2011;476(7360):298-303.
120. Lohr JG, Stojanov P, Lawrence MS, Auclair D, Chapuy B, Sougnez C, Cruz-Gordillo P, Knoechel B, Asmann YW, Slager SL and others. Discovery and prioritization of somatic mutations in diffuse large B-cell lymphoma (DLBCL) by whole-exome sequencing. Proc Natl Acad Sci U S A 2012;109(10):3879-84.
121. Malina A, Mills JR, Cencic R, Yan Y, Fraser J, Schippers LM, Paquet M, Dostie J, Pelletier J. Repurposing CRISPR/Cas9 for in situ functional assays. Genes & development 2013;27(23):2602-14.
122. Eischen CM, Weber JD, Roussel MF, Sherr CJ, Cleveland JL. Disruption of the ARF-Mdm2-p53 tumor suppressor pathway in Myc-induced lymphomagenesis. Genes & development 1999;13(20):2658-69.
123. Conner DA. Mouse embryo fibroblast (MEF) feeder cell preparation. Curr Protoc Mol Biol 2001;Chapter 23:Unit 23 2.
124. Davis HE, Morgan JR, Yarmush ML. Polybrene increases retrovirus gene transfer efficiency by enhancing receptor-independent virus adsorption on target cell membranes. Biophys Chem 2002;97(2-3):159-72.
125. Bosma M, Schuler W, Bosma G. The scid mouse mutant. Curr Top Microbiol Immunol 1988;137:197-202.
126. Takizawa Y, Saida T, Tokuda Y, Dohi S, Wang YL, Urano K, Hioki K, Ueyama Y. New immunodeficient (nude-scid, beige-scid) mice as excellent recipients of human skin grafts containing intraepidermal neoplasms. Arch Dermatol Res 1997;289(4):213-8.
127. Hulspas R. Titration of fluorochrome-conjugated antibodies for labeling cell surface markers on live cells. Curr Protoc Cytom 2010;Chapter 6:Unit 6 29.
128. Baumgarth N, Roederer M. A practical approach to multicolor flow cytometry for immunophenotyping. J Immunol Methods 2000;243(1-2):77-97.
129. Maecker HT, Trotter J. Flow cytometry controls, instrument setup, and the determination of positivity. Cytometry A 2006;69(9):1037-42.
130. Nielsen TH, Diaz Z, Christodoulopoulos R, Charbonneau F, Qureshi S, Rousseau C, Benlimame N, Camlioglu E, Constantin AM, Oros KK and others. Methods for sample acquisition and processing of serial blood and tumor biopsies for multicenter diffuse large B-cell lymphoma clinical trials. Cancer epidemiology, biomarkers & prevention : a publication of the American Association for Cancer Research, cosponsored by the American Society of Preventive Oncology 2014;23(12):2688-93.
131. Wright G, Tan B, Rosenwald A, Hurt EH, Wiestner A, Staudt LM. A gene expression-based method to diagnose clinically distinct subgroups of diffuse large B cell lymphoma. Proc Natl Acad Sci U S A 2003;100(17):9991-6.
132. Geiss GK, Bumgarner RE, Birditt B, Dahl T, Dowidar N, Dunaway DL, Fell HP, Ferree S, George RD, Grogan T and others. Direct multiplexed measurement of gene expression with color-coded probe pairs. Nature biotechnology 2008;26(3):317-25.
133. Subramanian A, Tamayo P, Mootha VK, Mukherjee S, Ebert BL, Gillette MA, Paulovich A, Pomeroy SL, Golub TR, Lander ES and others. Gene set enrichment analysis: a

knowledge-based approach for interpreting genome-wide expression profiles. Proc Natl Acad Sci U S A 2005;102(43):15545-50.
134. Mootha VK, Lindgren CM, Eriksson KF, Subramanian A, Sihag S, Lehar J, Puigserver P, Carlsson E, Ridderstrale M, Laurila E and others. PGC-1alpha-responsive genes involved in oxidative phosphorylation are coordinately downregulated in human diabetes. Nat Genet 2003;34(3):267-73.
135. Schmitt CA, Lowe SW. Bcl-2 mediates chemoresistance in matched pairs of primary E(mu)-myc lymphomas in vivo. Blood cells, molecules & diseases 2001;27(1):206-16.
136. Schuster C, Berger A, Hoelzl MA, Putz EM, Frenzel A, Simma O, Moritz N, Hoelbl A, Kovacic B, Freissmuth M and others. The cooperating mutation or "second hit" determines the immunologic visibility toward MYC-induced murine lymphomas. Blood 2011;118(17):4635-45.
137. Harris AW, Pinkert CA, Crawford M, Langdon WY, Brinster RL, Adams JM. The E mu-myc transgenic mouse. A model for high-incidence spontaneous lymphoma and leukemia of early B cells. J Exp Med 1988;167(2):353-71.
138. Schmitt CA, Lowe SW. Apoptosis and chemoresistance in transgenic cancer models. Journal of molecular medicine 2002;80(3):137-46.
139. Brode S, Cooke A. Immune-potentiating effects of the chemotherapeutic drug cyclophosphamide. Crit Rev Immunol 2008;28(2):109-26.
140. Lambert C, Desbarats J. The anti-Fas antibody M-20 cross-reacts with intracellular proteins: implications for false-positive detection of Fas. Apoptosis 2007;12(2):459-62.
141. Schmitz I, Krueger A, Baumann S, Kirchhoff S, Krammer PH. Specificity of anti-human CD95 (APO-1/Fas) antibodies. Biochem Biophys Res Commun 2002;297(3):459-62.
142. Houdebine LM, Attal J. Internal ribosome entry sites (IRESs): reality and use. Transgenic Res 1999;8(3):157-77.
143. Chen L, Park SM, Tumanov AV, Hau A, Sawada K, Feig C, Turner JR, Fu YX, Romero IL, Lengyel E and others. CD95 promotes tumour growth. Nature 2010;465(7297):492-6.
144. Prelich G. Gene overexpression: uses, mechanisms, and interpretation. Genetics 2012;190(3):841-54.
145. Waldhauer I, Steinle A. NK cells and cancer immunosurveillance. Oncogene 2008;27(45):5932-43.
146. Galluzzi L, Senovilla L, Zitvogel L, Kroemer G. The secret ally: immunostimulation by anticancer drugs. Nature reviews. Drug discovery 2012;11(3):215-33.
147. Zitvogel L, Apetoh L, Ghiringhelli F, Kroemer G. Immunological aspects of cancer chemotherapy. Nature reviews. Immunology 2008;8(1):59-73.
148. Vega MI, Huerta-Yepez S, Jazirehi AR, Garban H, Bonavida B. Rituximab (chimeric anti-CD20) sensitizes B-NHL cell lines to Fas-induced apoptosis. Oncogene 2005;24(55):8114-27.
149. Bennett M, Macdonald K, Chan SW, Luzio JP, Simari R, Weissberg P. Cell surface trafficking of Fas: a rapid mechanism of p53-mediated apoptosis. Science 1998;282(5387):290-3.
150. Micheau O, Solary E, Hammann A, Martin F, Dimanche-Boitrel MT. Sensitization of cancer cells treated with cytotoxic drugs to fas-mediated cytotoxicity. Journal of the National Cancer Institute 1997;89(11):783-9.
151. Mizutani Y, Okada Y, Yoshida O, Fukumoto M, Bonavida B. Doxorubicin sensitizes human bladder carcinoma cells to Fas-mediated cytotoxicity. Cancer 1997;79(6):1180-9.

152. Newton K, Strasser A. Ionizing radiation and chemotherapeutic drugs induce apoptosis in lymphocytes in the absence of Fas or FADD/MORT1 signaling. Implications for cancer therapy. The Journal of experimental medicine 2000;191(1):195-200.
153. Lindner S, Dahlke K, Sontheimer K, Hagn M, Kaltenmeier C, Barth TF, Beyer T, Reister F, Fabricius D, Lotfi R and others. Interleukin 21-induced granzyme B-expressing B cells infiltrate tumors and regulate T cells. Cancer Res 2013;73(8):2468-79.
154. Hagn M, Jahrsdörfer B. Why do human B cells secrete granzyme B? Insights into a novel B-cell differentiation pathway. Oncoimmunology 2012;1(8):1368-1375.
155. Hagn M, Sontheimer K, Dahlke K, Brueggemann S, Kaltenmeier C, Beyer T, Hofmann S, Lunov O, Barth TF, Fabricius D and others. Human B cells differentiate into granzyme B-secreting cytotoxic B lymphocytes upon incomplete T-cell help. Immunol Cell Biol 2012;90(4):457-67.
156. Ranheim EA, Cantwell MJ, Kipps TJ. Expression of CD27 and its ligand, CD70, on chronic lymphocytic leukemia B cells. Blood 1995;85(12):3556-65.
157. Ryan MC, Kostner H, Gordon KA, Duniho S, Sutherland MK, Yu C, Kim KM, Nesterova A, Anderson M, McEarchern JA and others. Targeting pancreatic and ovarian carcinomas using the auristatin-based anti-CD70 antibody-drug conjugate SGN-75. Br J Cancer 2010;103(5):676-84.
158. Yang ZZ, Novak AJ, Ziesmer SC, Witzig TE, Ansell SM. CD70+ non-Hodgkin lymphoma B cells induce Foxp3 expression and regulatory function in intratumoral CD4+CD25 T cells. Blood 2007;110(7):2537-44.
159. Wischhusen J, Jung G, Radovanovic I, Beier C, Steinbach JP, Rimner A, Huang H, Schulz JB, Ohgaki H, Aguzzi A and others. Identification of CD70-mediated apoptosis of immune effector cells as a novel immune escape pathway of human glioblastoma. Cancer Res 2002;62(9):2592-9.
160. Soengas MS, Alarcon RM, Yoshida H, Giaccia AJ, Hakem R, Mak TW, Lowe SW. Apaf-1 and caspase-9 in p53-dependent apoptosis and tumor inhibition. Science 1999;284(5411):156-9.
161. Lossos IS, Natkunam Y, Levy R, Lopez CD. Apoptosis stimulating protein of p53 (ASPP2) expression differs in diffuse large B-cell and follicular center lymphoma: correlation with clinical outcome. Leuk Lymphoma 2002;43(12):2309-17.
162. Edinger M, Cao YA, Hornig YS, Jenkins DE, Verneris MR, Bachmann MH, Negrin RS, Contag CH. Advancing animal models of neoplasia through in vivo bioluminescence imaging. Eur J Cancer 2002;38(16):2128-36.
163. Contag CH, Jenkins D, Contag PR, Negrin RS. Use of reporter genes for optical measurements of neoplastic disease in vivo. Neoplasia 2000;2(1-2):41-52.
164. Hutchens M, Luker GD. Applications of bioluminescence imaging to the study of infectious diseases. Cell Microbiol 2007;9(10):2315-22.
165. Inoue Y, Kiryu S, Izawa K, Watanabe M, Tojo A, Ohtomo K. Comparison of subcutaneous and intraperitoneal injection of D-luciferin for in vivo bioluminescence imaging. Eur J Nucl Med Mol Imaging 2009;36(5):771-9.
166. Hoffman RM. Advantages of multi-color fluorescent proteins for whole-body and in vivo cellular imaging. J Biomed Opt 2005;10(4):41202.
167. Leblond F, Davis SC, Valdes PA, Pogue BW. Pre-clinical whole-body fluorescence imaging: Review of instruments, methods and applications. J Photochem Photobiol B 2010;98(1):77-94.

168. Shcherbo D, Merzlyak EM, Chepurnykh TV, Fradkov AF, Ermakova GV, Solovieva EA, Lukyanov KA, Bogdanova EA, Zaraisky AG, Lukyanov S and others. Bright far-red fluorescent protein for whole-body imaging. Nat Methods 2007;4(9):741-6.
169. Cho KH, Lee JS, Choi YD, Boo KS. Structural polymorphism of the luciferase gene in the firefly, Luciola lateralis. Insect Mol Biol 1999;8(2):193-200.
170. Burgos JS, Rosol M, Moats RA, Khankaldyyan V, Kohn DB, Nelson MD, Jr., Laug WE. Time course of bioluminescent signal in orthotopic and heterotopic brain tumors in nude mice. Biotechniques 2003;34(6):1184-8.
171. Inoue Y, Kiryu S, Watanabe M, Tojo A, Ohtomo K. Timing of imaging after d-luciferin injection affects the longitudinal assessment of tumor growth using in vivo bioluminescence imaging. Int J Biomed Imaging 2010;2010:471408.
172. Ito K, Smith BR, Parashurama N, Yoon JK, Song SY, Miething C, Mallick P, Lowe S, Gambhir SS. Unexpected dissemination patterns in lymphoma progression revealed by serial imaging within a murine lymph node. Cancer Res 2012;72(23):6111-8.
173. Zitvogel L, Kepp O, Senovilla L, Menger L, Chaput N, Kroemer G. Immunogenic tumor cell death for optimal anticancer therapy: the calreticulin exposure pathway. Clin Cancer Res 2010;16(12):3100-4.

Supplemental Table 1: List of immune-related genes tested by Nanostring

ABL1	CASP6	IRF2	PPP3R2
AKT1	CASP7	IRF3	PRF1
AKT2	CASP8	IRF4	PRKACA
AKT3	CASP9	IRF5	PRKACB
APAF1	CD40	IRF6	PRKACG
ATM	CD40LG	IRF7	PRKAR1A
BAD	CD70	JUN	PRKAR2A
BAG1	CFLAR	LMNA	PRKAR2B
BAG3	CHP	LMNB1	PYCARD
BAG4	CHUK	LTA	RELA
BAK1	CIDEA	LTBR	RELB
BAX	CIDEB	MAP2K4	RIPK1
BCL10	CRADD	MAP3K1	RIPK2
BCL2	CSF2RB	MAP3K14	SFRS2IP
BCL2A1	CYCS	MAPK10	STAT1
BCL2L1	DAPK1	MCL1	TFG
BCL2L11	DAXX	MDM2	TNF
BCL2L2	FADD	MYC	TNFRSF10A
BCLAF1	FAS	MYD88	TNFRSF10B
BFAR	FASLG	NFKB1	TNFRSF10C
BID	GADD45A	NFKB2	TNFRSF10D
BIK	GZMB	NFKBIA	TNFRSF11B
BIRC2	HELLS	NFKBIE	TNFRSF1A
BIRC3	HMGB1	NGFB	TNFRSF1B
BIRC5	HMGB2	NGFR	TNFRSF21
BIRC6	HRK	NR3C1	TNFRSF25
BIRC8	IGF1R	NTRK1	TNFRSF9
BNIP2	IKBKB	PARP1	TNFSF10
BNIP3	IKBKE	PIK3CA	TNFSF8
BNIP3L	IKBKG	PIK3CB	TOP2A
BOK	IL1A	PIK3CD	TOP2B
BRAF	IL1B	PIK3CG	TP53
CARD6	IL1R1	PIK3R1	TP53BP2
CARD8	IL1RAP	PIK3R2	TP73
CASP1	IL3	PIK3R3	TRADD
CASP10	IL3RA	PIK3R5	TRAF1
CASP14	IRAK1	PPP3CA	TRAF2
CASP2	IRAK2	PPP3CB	TRAF3
CASP3	IRAK3	PPP3CC	TRAF6
CASP4	IRAK4	PPP3R1	XIAP
CASP5	IRF1		